WashU

In collaboration with Bhupal Dev, Christian Lopez and Vishvas Pandey [2605.XXXXX]

Form Factor Uncertainty Analysis for Coherent Neutrino Trident Scattering

Phenomenology 2026 Symposium

University of Pittsburgh

May 11, 2026

Diego Lopez Gutierrez

Neutrino Tridents $\nu_\ell N \to \nu_{\ell'} \ell \ell' N$

- $\nu_\mu N \to \nu_\mu \mu^+ \mu^- N$: Charm-II (~55), CCFR (~37); NuTeV. Consistent with SM.

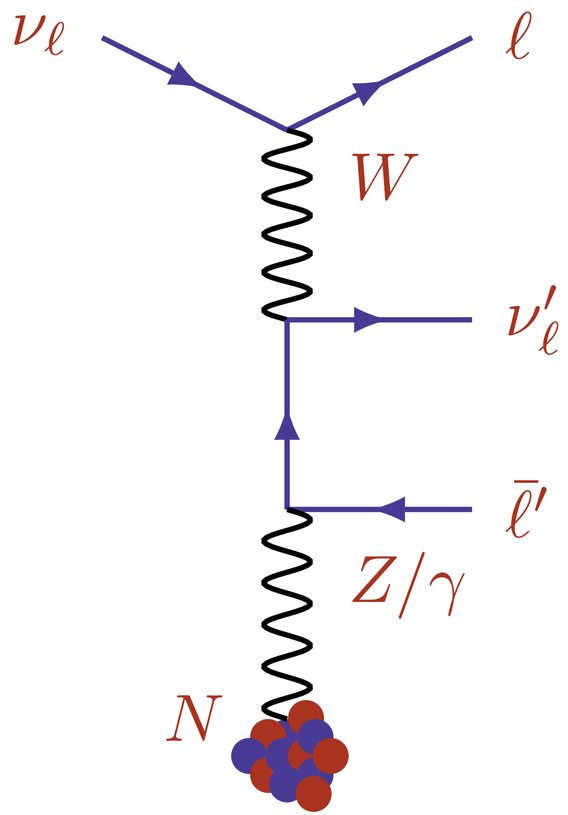

Charged Current

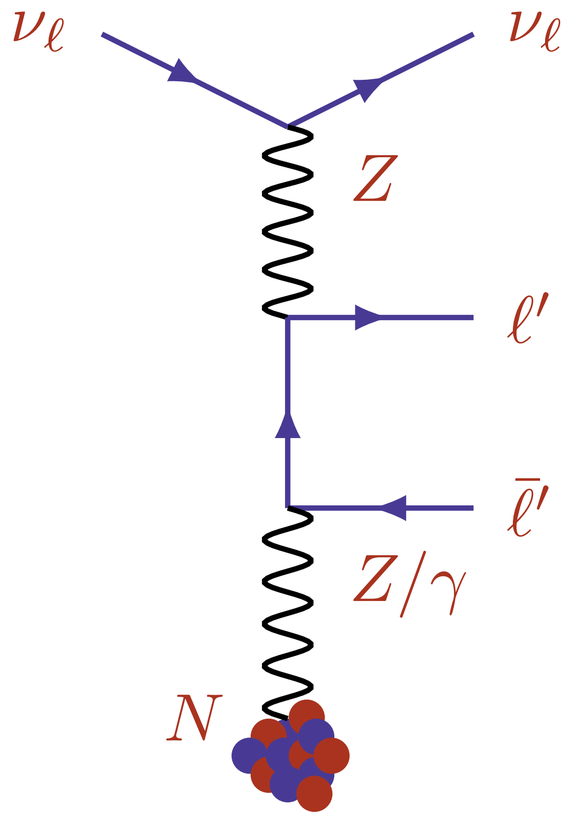

Neutral Current

Neutrino Tridents $\nu_\ell N \to \nu_{\ell'} \ell \ell' N$

- $\nu_\mu N \to \nu_\mu \mu^+ \mu^- N$: Charm-II (~55), CCFR (~37); NuTeV. Consistent with SM.

- Precision neutrino physics:
  - $\mathcal{O}(1000)$ at DUNE alone and $\mathcal{O}(100)$ at other accelerator neutrino experiments, compared to $\lesssim 100$ tridents ever detected so far!

TABLE II. Expected number of muon-neutrino-induced Standard Model trident events at the DUNE near detector per tonne of argon and year of operation in neutrino mode (first four rows) or antineutrino mode (last four rows). The numbers in parenthesis correspond to the total statistics in the 147-tonne LArTPC for a run of 3 years.

	Coherent	Incoherent
$\nu_\mu \to \nu_\mu \mu^+ \mu^-$	1.17 ± 0.07 (516 ± 31)	0.49 ± 0.15 (216 ± 66)
$\nu_\mu \to \nu_\mu e^+ e^-$	2.84 ± 0.17 (1252 ± 75)	0.18 ± 0.06 (79 ± 27)
$\nu_\mu \to \nu_e e^+ \mu^-$	9.8 ± 0.6 (4322 ± 265)	1.2 ± 0.4 (529 ± 176)
$\nu_\mu \to \nu_e \mu^+ e^-$	0 (0)	0 (0)
$\bar{\nu}_\mu \to \bar{\nu}_\mu \mu^+ \mu^-$	0.72 ± 0.04 (318 ± 18)	0.32 ± 0.10 (141 ± 44)
$\bar{\nu}_\mu \to \bar{\nu}_\mu e^+ e^-$	2.21 ± 0.13 (975 ± 57)	0.13 ± 0.04 (57 ± 18)
$\bar{\nu}_\mu \to \bar{\nu}_e e^+ \mu^-$	0 (0)	0 (0)
$\bar{\nu}_\mu \to \bar{\nu}_e \mu^+ e^-$	7.0 ± 0.4 (3087 ± 176)	0.9 ± 0.3 (397 ± 132)

Altmannshofer et al. [1902.06765]

Neutrino Tridents $\nu_\ell N \to \nu_{\ell'} \ell \ell' N$

- $\nu_\mu N \to \nu_\mu \mu^+ \mu^- N$: Charm-II (~55), CCFR (~37); NuTeV. Consistent with SM.

- Precision neutrino physics:
  - $\mathcal{O}(1000)$ at DUNE alone and $\mathcal{O}(100)$ at other accelerator neutrino experiments, compared to $\lesssim 100$ tridents ever detected so far!

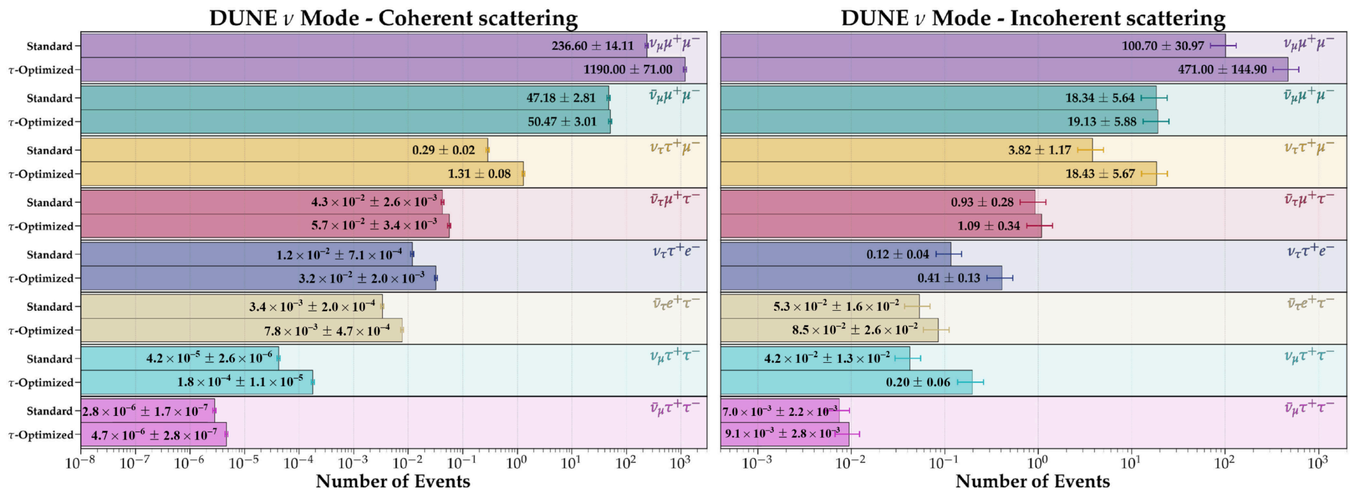

Bigaran, DLG, et al.[2406.20067]

FIG. 3. Number of trident events from coherent (left) and incoherent (right) scattering at DUNE near detector with 67 ton of argon and 3.3×10^{21} POT in the forward horn current mode for both standard and tau-optimized fluxes.

Channel	T2K-I	T2K-II	MINOS	MINOS+	NOνA-I	NOνA-II	MINERνA
$\nu_\mu \to \nu_e e^+ \mu^-$	538	1379	179 (25)	688	71 (14)	291 (73)	140 (13)
	49	126	21 (3)	82	21 (4)	86 (21)	30 (3)
$\overline{\nu}_\mu \to \overline{\nu}_e e^- \mu^+$	23	58	42 (31)	38	10 (57)	41 (296)	8 (89)
	2	5	5 (4)	5	3 (17)	12 (88)	2 (19)
$\nu_e \to \nu_\mu e^- \mu^+$	2	6	1 (0.2)	4	2 (0.5)	8 (3)	1 (0.09)
	0.3	1	0.3 (0.04)	0.8	0.9 (0.2)	4 (1)	0.3 (0.03)
$\overline{\nu}_e \to \overline{\nu}_\mu e^+ \mu^-$	0.2	0.6	0.4 (0.3)	0.4	0.5 (0.9)	2 (5)	0.06 (0.5)
	0.04	0.1	0.08 (0.06)	0.08	0.2 (0.4)	0.8 (2)	0.02 (0.2)
Total $e^\pm \mu^\mp$	563	1444	222 (56)	730	83 (72)	340 (374)	149 (102)
	52	132	27 (7)	88	25 (22)	102 (114)	32 (22)
$\nu_\mu \to \nu_\mu e^+ e^-$	257	659	48 (5)	44	22 (3)	90 (16)	35 (3)
	9	23	3 (0.4)	3	3 (0.6)	00	4 (0.4)
$\overline{\nu}_\mu \to \overline{\nu}_\mu e^- e^+$	10	26	9 (8)	9	2 (16)	8 (83)	2 (23)
	0.4	1	0.7 (0.5)	0.7	0.4 (3)	2 (15)	0.2 (3)
$\nu_e \to \nu_e e^- e^+$	9	24	3 (0.3)	8	3 (0.9)	12 (5)	2 (0.2)
	0.3	0.8	0.2 (0.03)	0.6	0.7 (0.2)	3 (1)	0.2 (0.02)
$\overline{\nu}_e \to \overline{\nu}_e e^+ e^-$	0.9	2	0.7 (0.6)	0.7	0.8 (2)	3 (10)	0.1 (0.9)
	0.03	0.08	0.06 (0.04)	0.05	0.2 (0.3)	0.8 (1)	0.01 (0.1)
Total $e^+ e^-$	277	711	61 (15)	62	29 (22)	119 (114)	39 (27)
	10	25	4 (1)	4	4 (4)	16 (21)	4 (3)
$\nu_\mu \to \nu_\mu \mu^+ \mu^-$	29	73	21 (3)	81	7 (2)	28 (11)	17 (2)
	15	38	8 (1)	33	7 (2)	29 (10)	12 (1)
$\overline{\nu}_\mu \to \overline{\nu}_\mu \mu^- \mu^+$	1	3	5 (3)	5	1 (7)	4 (35)	1 (11)
	0.7	2	2 (1)	2	1 (6)	4 (30)	0.7 (8)
$\nu_e \to \nu_e \mu^+ \mu^-$	0.09	0.2	0.09 (0.01)	0.3	0.1 (0.04)	0.4 (0.2)	0.06 (0.007)
	0.04	0.1	0.03 (0.004)	0.1	0.1 (0.03)	0.4 (0.1)	0.03 (0.004)
$\overline{\nu}_e \to \overline{\nu}_e \mu^+ \mu^-$	0.01	0.03	0.03 (0.02)	0.03	0.04 (0.06)	0.2 (0.3)	0.004 (0.03)
	0.004	0.01	0.01 (0.009)	0.01	0.03(0.05)	0.1 (0.3)	0.003 (0.02)
Total $\mu^+ \mu^-$	30	76	26 (6)	86	9 (9)	37 (47)	18 (13)
	16	40	10 (2)	35	8 (8)	34 (36)	13 (9)

Ballett et al. [1807.10973]

Table 7. Total number of *coherent* (top row) and *diffractive* (bottom row) trident events expected at different non-LAr detectors for each channel. The numbers in parentheses are for the antineutrino running mode, when present. These calculations consider a detection efficiency of 100%.

Neutrino Tridents $\nu_\ell N \to \nu_{\ell'} \ell \ell' N$

- $\nu_\mu N \to \nu_\mu \mu^+ \mu^- N$: Charm-II (~55), CCFR (~37); NuTeV. Consistent with SM.

- Precision neutrino physics:
  - $\mathcal{O}(1000)$ at DUNE alone and $\mathcal{O}(100)$ at other accelerator neutrino experiments, compared to $\lesssim 100$ tridents ever detected so far!
  - Unique probe of EW interactions and ν-phillic BSM mediators.

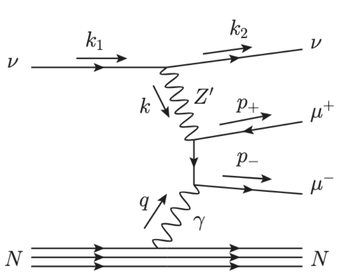

FIG. 1. The leading order contribution of the Z′ to neutrino trident production (another diagram with μ^+ and μ^- reversed is not shown). Other contributions at the same order in g' are further suppressed by the Fermi scale.

Altmannshofer et al. [1406.2332]

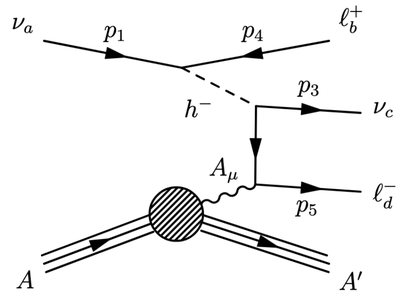

FIG. 1: Neutrino trident production of a charged Weyl lepton pair via a new charged scalar. There are three additional diagrams that can be obtained. The two charged leptons can be of different flavours. The connecting photon can interact with the nucleus (as shown above), or with individual nucleons.

Magill & Plestid [1710.08431]

Ballett et al. [1902.08579]

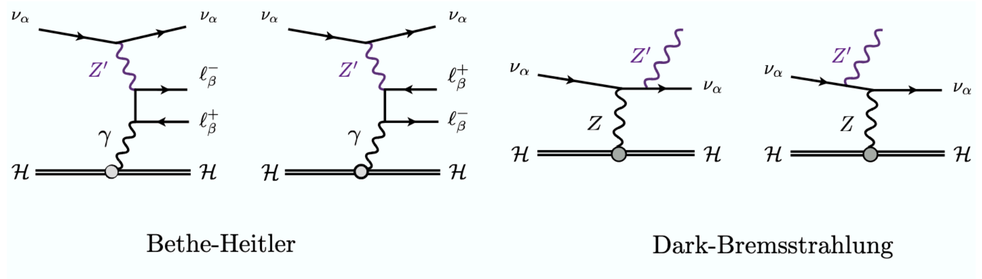

Figure 1. The BSM contributions to neutrino trident production considered in our calculation. The diagrams on the top row are referred to as Bether-Heitler contributions due to their resemblance to pair-production. On the bottom row, we show diagrams with a radiative-like Z' contribution, which allows for the production of on-shell Z' particles, which subsequently decays into the charged-lepton pair.

Neutrino Tridents $\nu_\ell N \to \nu_{\ell'} \ell \ell' N$

- $\nu_\mu N \to \nu_\mu \mu^+ \mu^- N$: Charm-II (~55), CCFR (~37); NuTeV. Consistent with SM.

- Precision neutrino physics:
  - $\mathcal{O}(1000)$ at DUNE alone and $\mathcal{O}(100)$ at other accelerator neutrino experiments, compared to $\lesssim 100$ tridents ever detected so far!
  - Unique probe of EW interactions and ν-phillic BSM mediators.

Accurate SM trident event rates are imperative for proper comparison with BSM predictions!

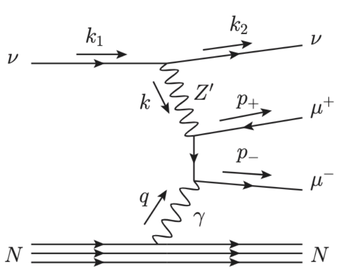

FIG. 1. The leading order contribution of the Z′ to neutrino trident production (another diagram with μ^+ and μ^- reversed is not shown). Other contributions at the same order in g' are further suppressed by the Fermi scale.

Altmannshofer et al. [1406.2332]

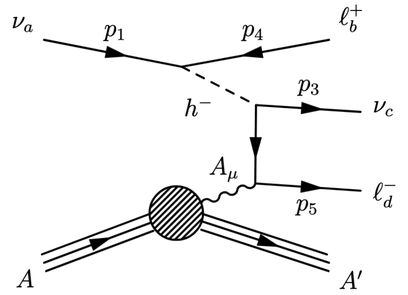

FIG. 1: Neutrino trident production of a charged Weyl lepton pair via a new charged scalar. There are three additional diagrams that can be obtained. The two charged leptons can be of different flavours. The connecting photon can interact with the nucleus (as shown above), or with individual nucleons.

Magill & Plestid [1710.08431]

Ballett et al. [1902.08579]

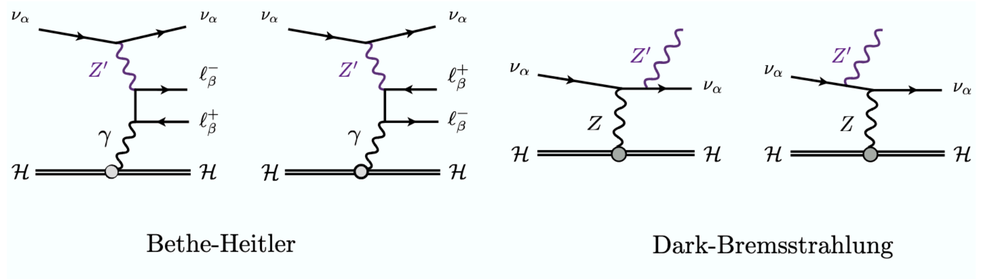

Figure 1. The BSM contributions to neutrino trident production considered in our calculation. The diagrams on the top row are referred to as Bether-Heitler contributions due to their resemblance to pair-production. On the bottom row, we show diagrams with a radiative-like Z' contribution, which allows for the production of on-shell Z' particles, which subsequently decays into the charged-lepton pair.

At accelerator neutrino experiments...

At accelerator neutrino experiments...

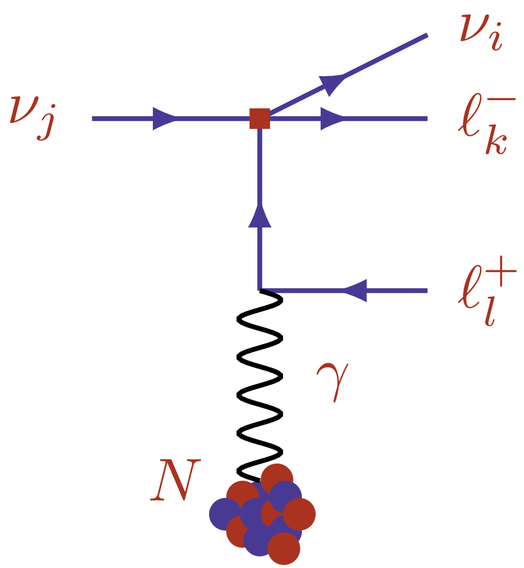

At accelerator neutrino experiments...

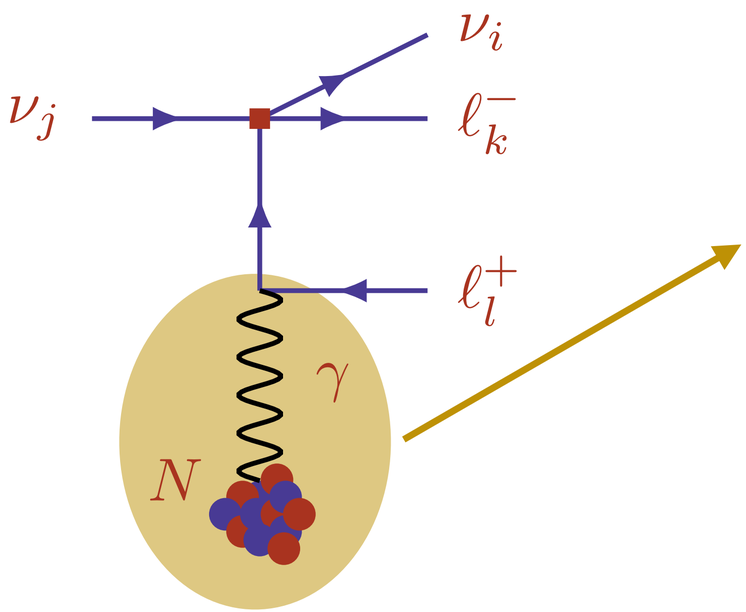

Coherent Scattering

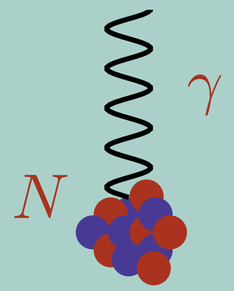

- Nuclear form factor.
- Z^2 scaling.
- $\ell^+\ell'^-$ final state.

At accelerator neutrino experiments...

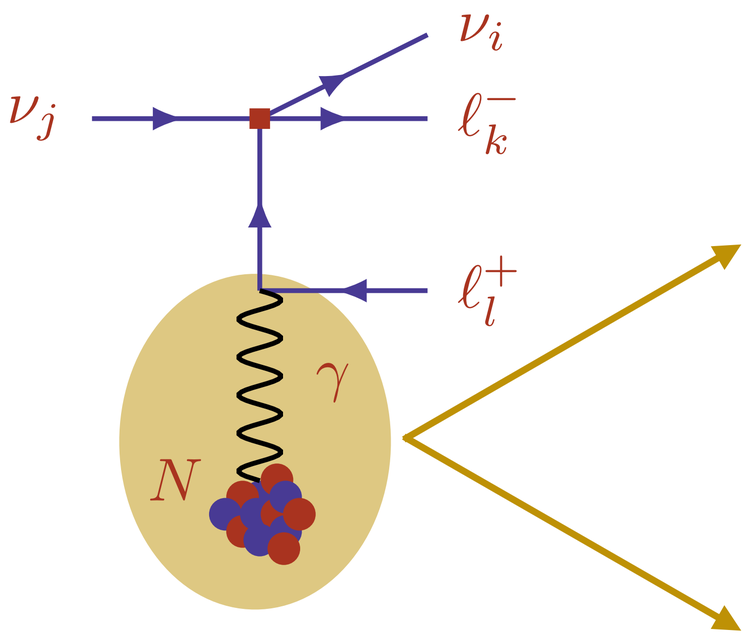

Coherent Scattering

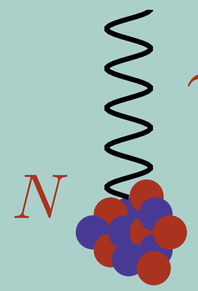

- Nuclear form factor.
- Z^2 scaling.
- $\ell^+\ell'^-$ final state.

Incoherent (diffractive) Scattering

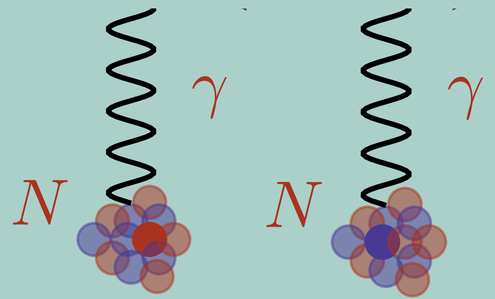

- Nucleon form factors.
- $2Z$ scaling.
- $\ell^+\ell'^- + p(n)$ final state.

Argon Charged Form Factor

Argon Charged Form Factor

No experimental data on the electromagnetic argon nuclear form factor since 1982!

ELSEVIER

Nuclear Physics A

Volume 379, Issue 3, 10 May 1982, Pages 396-406

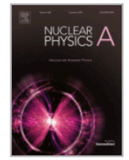

Elastic electron scattering from ^{40}Ar

C.R. Ottermann *, CH. Schmitt **, G.G. Simon **, F. Borkowski **, V.H. Walther

Institut für Kernphysik, Johannes Gutenberg-Universität, D-6500 Mainz, Federal Republic of Germany

Abstract

Cross sections for elastic electron scattering from ^{40}Ar have been measured for the momentum transfer range from 0.59 to 1.31 fm^{-1}. We have analyzed with the Fourier-Bessel ansatz our data as well as the data of former experiments. The rms charge radius we have found is 3.423(14) fm. The results are in excellent agreement with latest muonic data. Furthermore, we have reanalyzed former ^{40}Ca data and have discussed the ^{40}Ca-^{40}Ar charge distribution.

Argon Charged Form Factor

No experimental data on the electromagnetic argon nuclear form factor since 1982!

And current data only available for momentum transfers

$Q \sim 0.11 - 0.26\,\text{GeV}.$

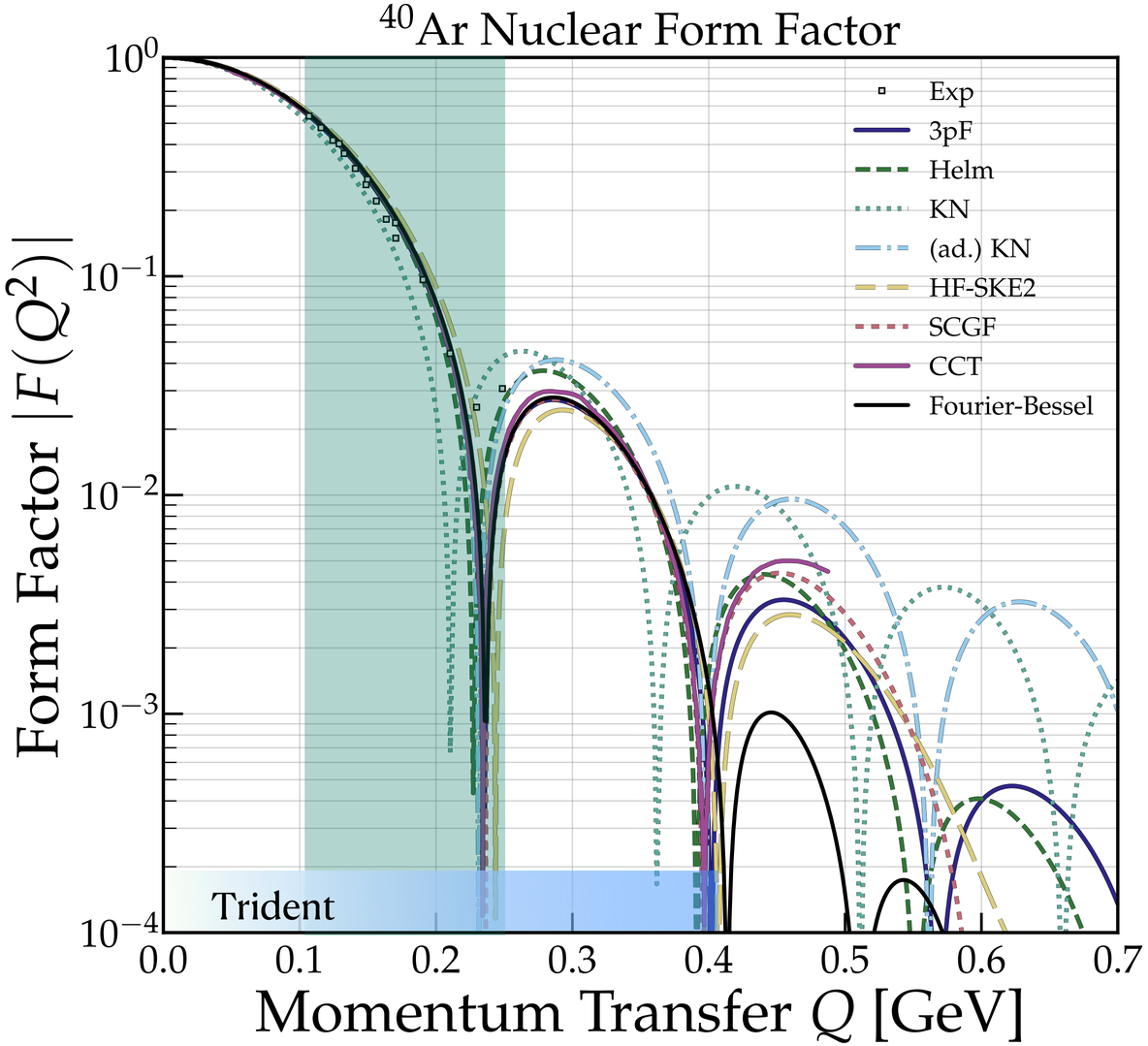

Argon Charged Form Factor

No experimental data on the electromagnetic argon nuclear form factor since 1982!

And current data only available for momentum transfers

$Q \sim 0.11 - 0.26\,\text{GeV}.$

Form factor uncertainty underestimated to be $\simeq 1\,\%$ * based only on Woods-Saxon parameterizations.

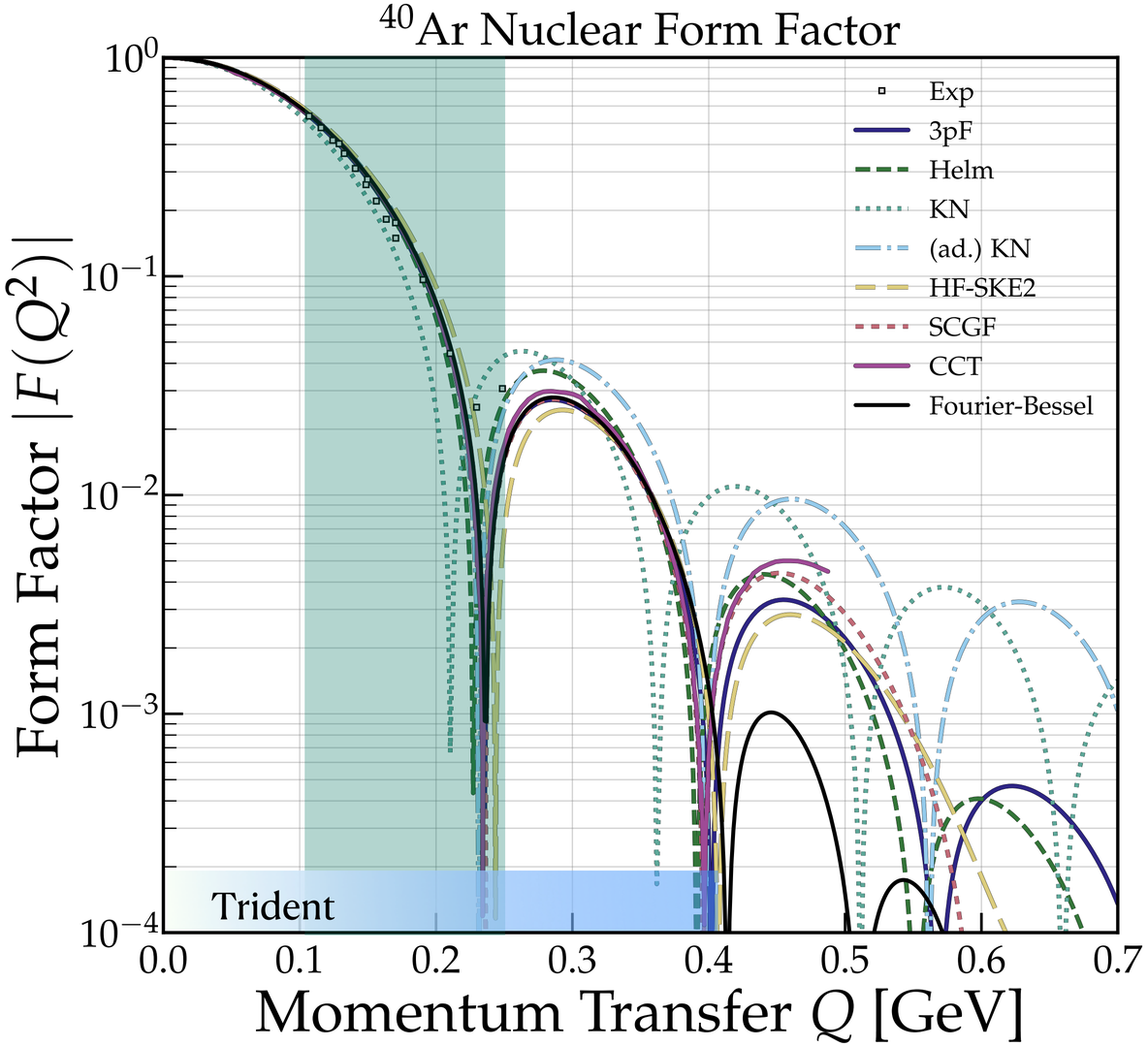

* Altmannshofer et al. [1902.06765]

Argon Charged Form Factor

- Woods-Saxon 3-parameter Fermi
  De Vries et al. [Atom. Data Nucl. Data Tabl. 1987]
- Helm
  Helm [Phys. Rev. 1956]
- Klein-Nystrand
  Klein & Nystrand [9902259]
- Adapted Klein-Nystrand
  Papoulias et al. [1911.00916]
- Hartree-Fock with Skyrme
  Van Dessel et al. [2007.03658]
- Coupled-cluster Theory
  Payne et al. [1908.09739]
- *Ab initio* Self-Consistent Green's Function
  Barbieri et al. [1907.01122]
- Fourier-Bessel
  De Vries et al. [Atom. Data Nucl. Data Tabl. 1987]

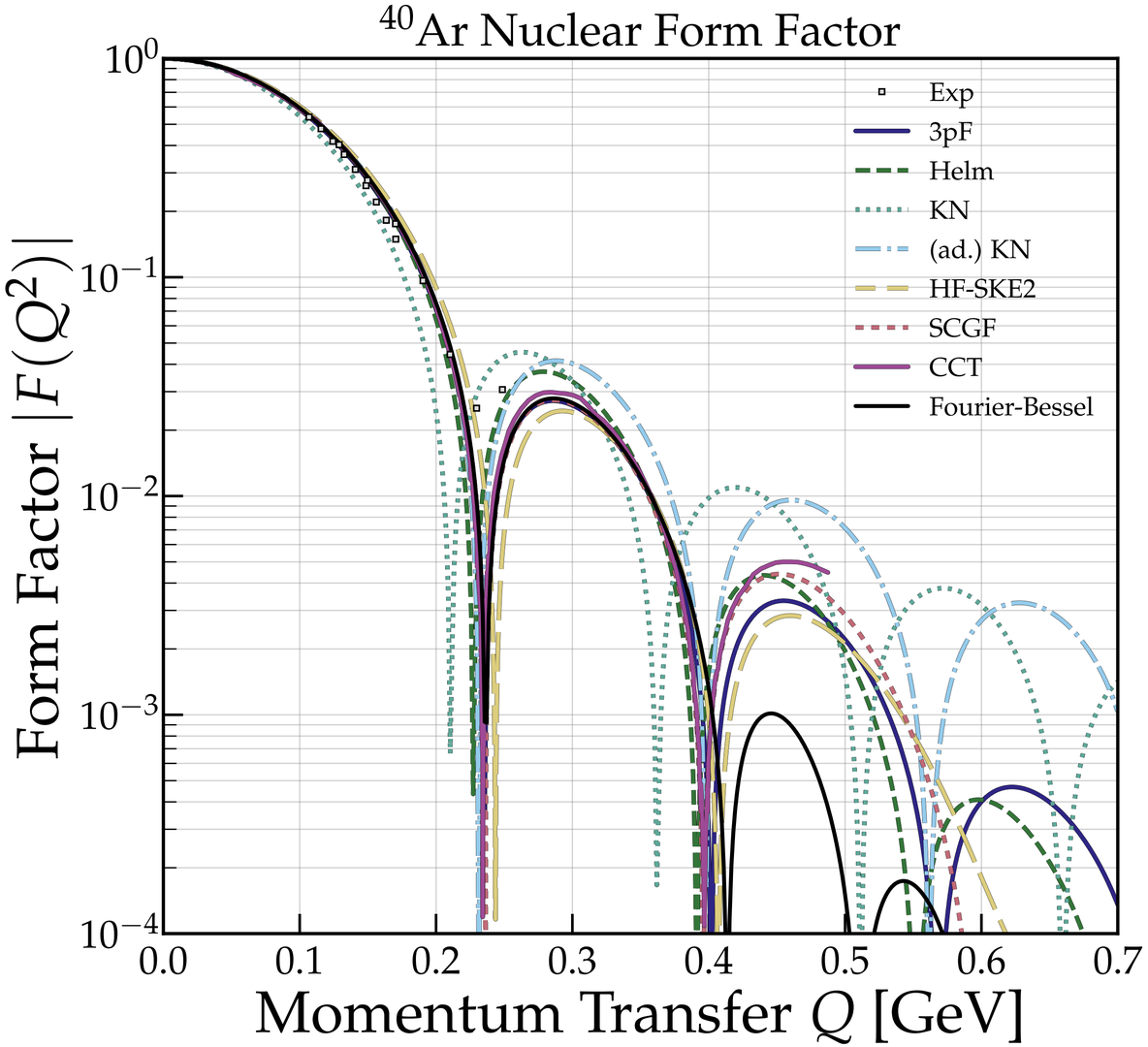

Argon Charged Form Factor

- Woods-Saxon 3-parameter Fermi
  De Vries et al. [Atom. Data Nucl. Data Tabl. 1987]
- Helm
  Helm [Phys. Rev. 1956]
- Klein-Nystrand
  Klein & Nystrand [9902259]
- Adapted Klein-Nystrand
  Papoulias et al. [1911.00916]
- Hartree-Fock with Skyrme
  Van Dessel et al. [2007.03658]
- Coupled-cluster Theory
  Payne et al. [1908.09739]
- *Ab initio* Self-Consistent Green's Function
  Barbieri et al. [1907.01122]
- Fourier-Bessel
  De Vries et al. [Atom. Data Nucl. Data Tabl. 1987]

How impactful can these differences be?

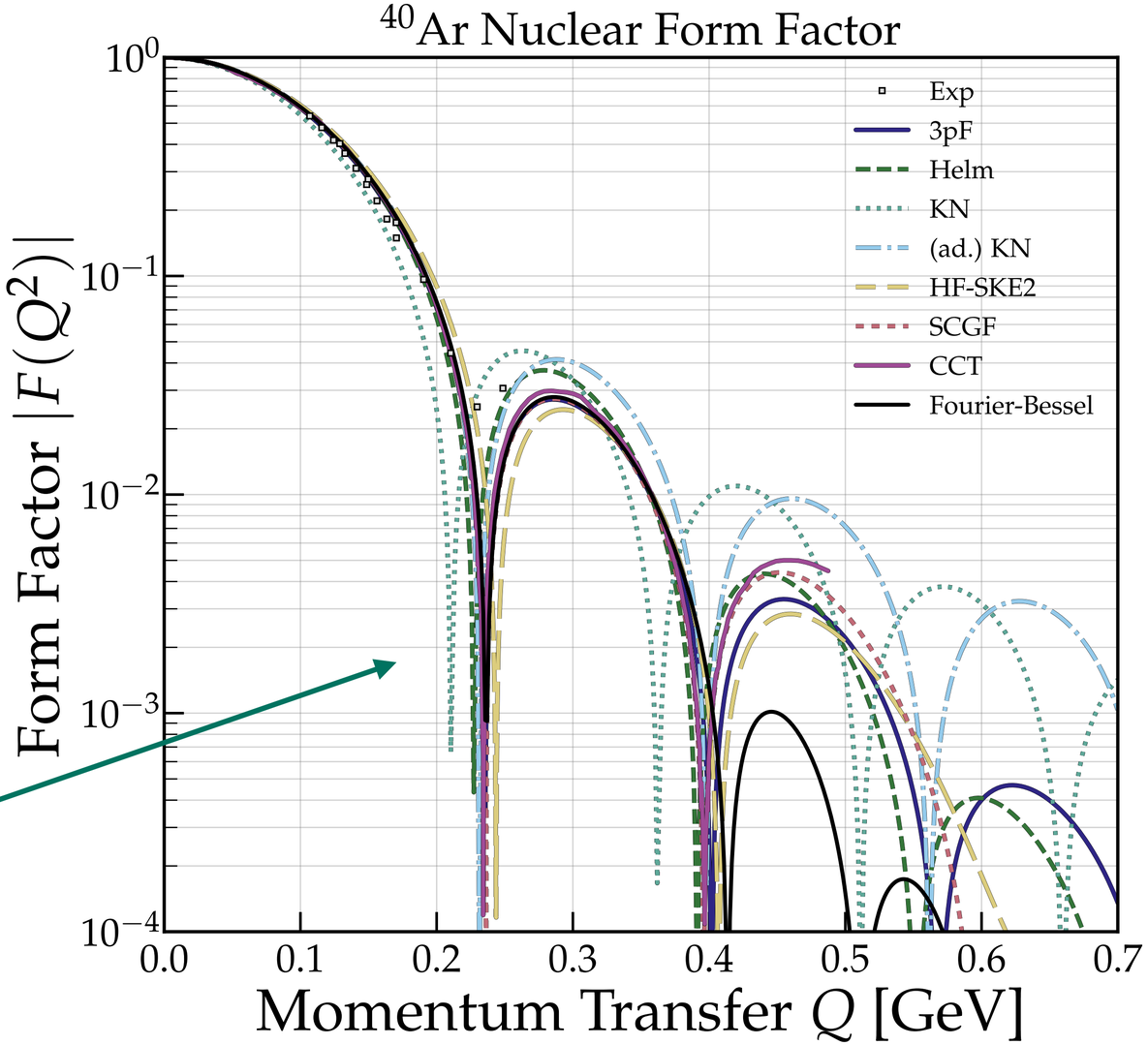

Cross Sections

Cross Sections

$$\mathrm{d}\sigma_{\mathrm{coh}} = \frac{Z^2 \alpha_{\mathrm{EM}}^2 G_F^2}{128\pi^6} \frac{1}{m_N E_\nu} \frac{\mathrm{d}^3 k'}{2E_{k'}} \frac{\mathrm{d}^3 p_+}{2E_+} \frac{\mathrm{d}^3 p_-}{2E_-} \frac{\mathrm{d}^3 P'}{2E_{P'}} \frac{H_N^{\alpha\beta} L_{\alpha\beta}}{q^4} \delta^4(k - k' - p_+ - p_- + q)$$

Cross Sections

$$\mathrm{d}\sigma_{\mathrm{coh}} = \frac{Z^2\alpha_{\mathrm{EM}}^2 G_F^2}{128\pi^6}\frac{1}{m_N E_\nu}\frac{\mathrm{d}^3k'}{2E_{k'}}\frac{\mathrm{d}^3p_+}{2E_+}\frac{\mathrm{d}^3p_-}{2E_-}\frac{\mathrm{d}^3P'}{2E_{P'}}\frac{H_N^{\alpha\beta}L_{\alpha\beta}}{q^4}\delta^4(k-k'-p_+-p_-+q)$$

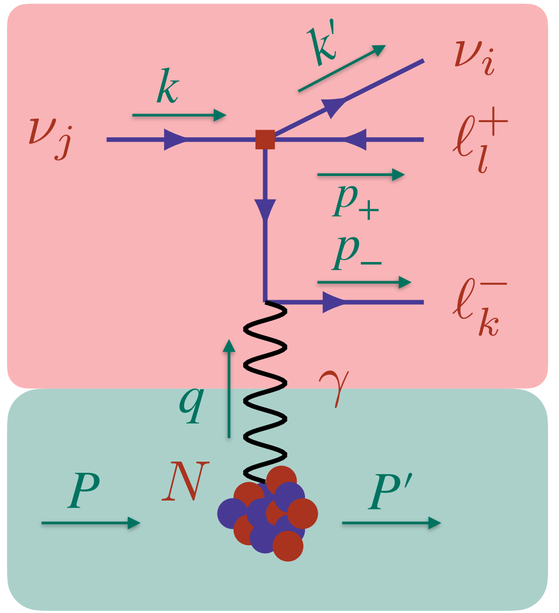

$$H_N^{\alpha\beta} = 4P^\alpha P^\beta [F_N(q^2)]^2$$

Cross Sections

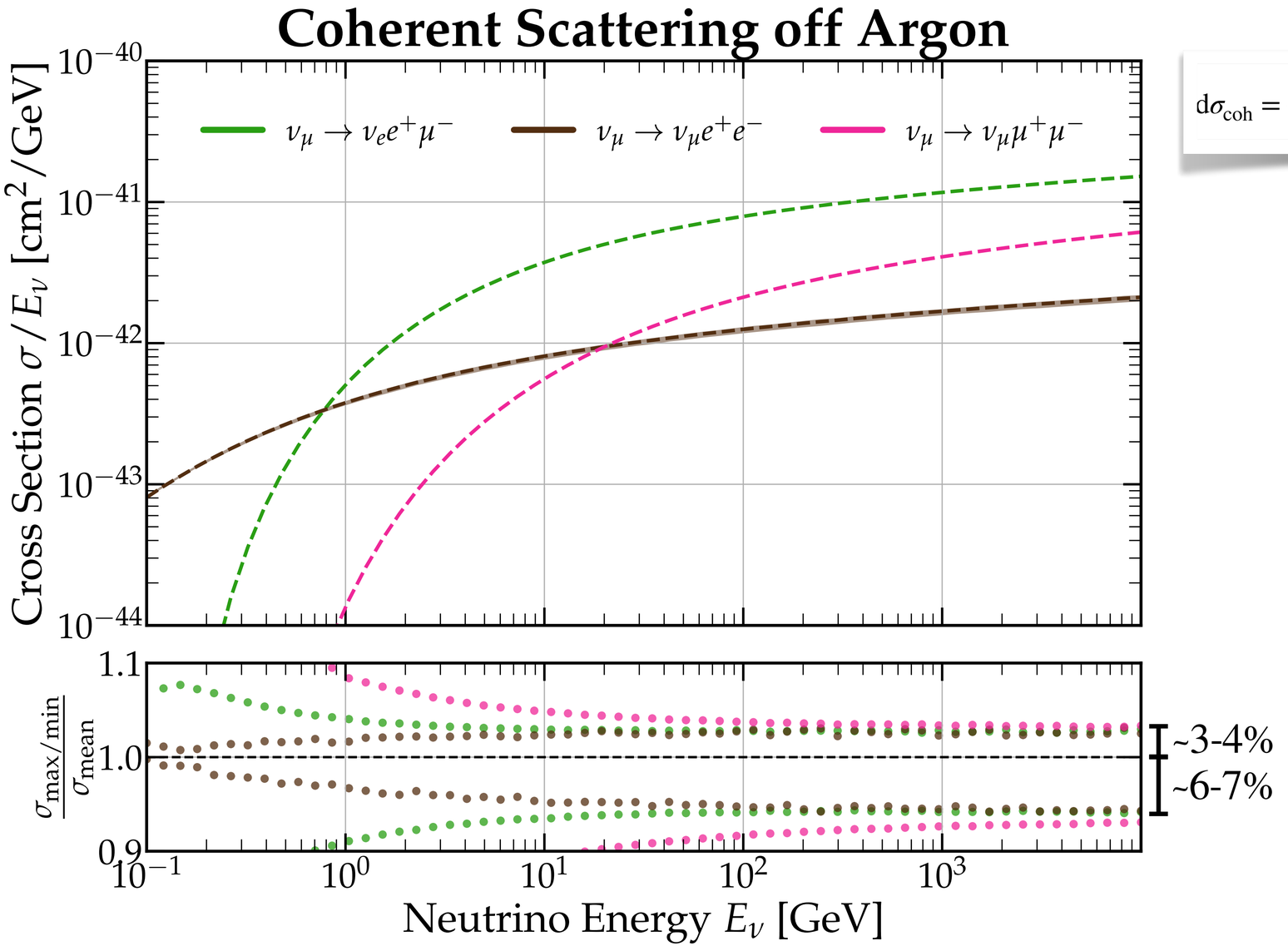

$$\mathrm{d}\sigma_{\mathrm{coh}} = \frac{Z^2 \alpha_{\mathrm{EM}}^2 G_F^2}{128\pi^6} \frac{1}{m_N E_\nu} \frac{\mathrm{d}^3 k'}{2E_{k'}} \frac{\mathrm{d}^3 p_+}{2E_+} \frac{\mathrm{d}^3 p_-}{2E_-} \frac{\mathrm{d}^3 P'}{2E_{P'}} \frac{H_N^{\alpha\beta} L_{\alpha\beta}}{q^4} \delta^4(k - k' - p_+ - p_- + q)$$

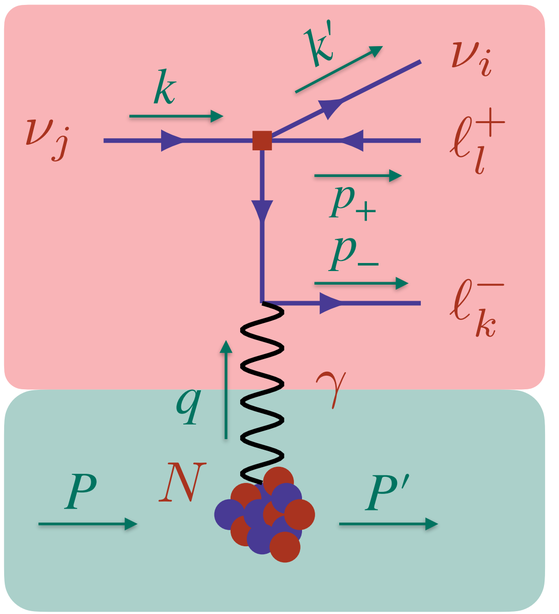

$$H_N^{\alpha\beta} = 4P^\alpha P^\beta [F_N(q^2)]^2$$

Event Rate

Event Rate

Number of nuclei

$$\frac{M_{\text{detector}}}{M_{\text{target}}}$$

Event Rate

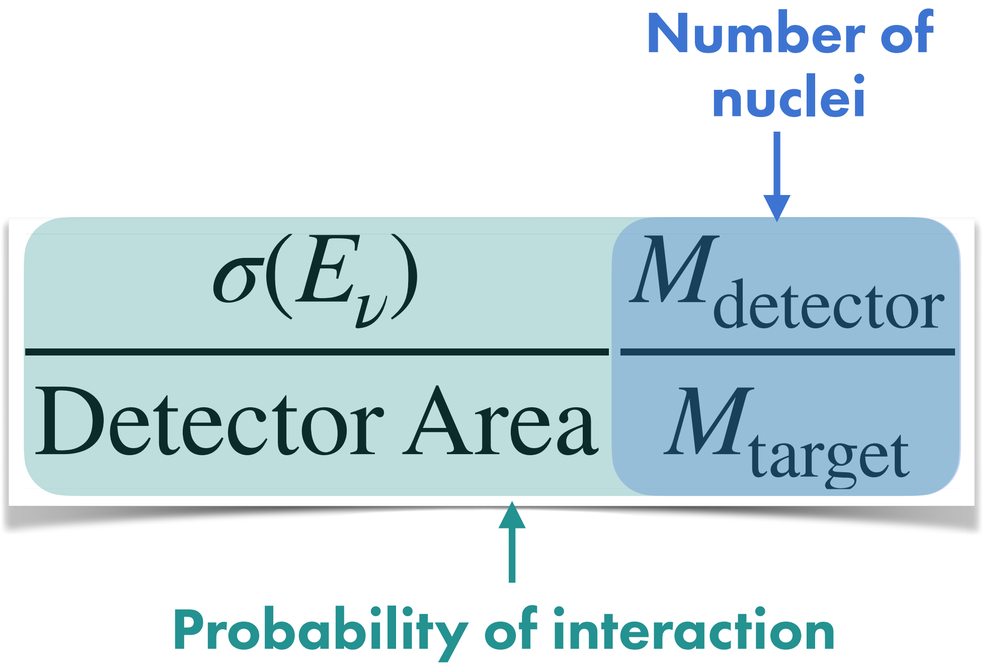
Number of nuclei
$\frac{\sigma(E_\nu)}{\text{Detector Area}} \frac{M_{\text{detector}}}{M_{\text{target}}}$
Probability of interaction

Event Rate

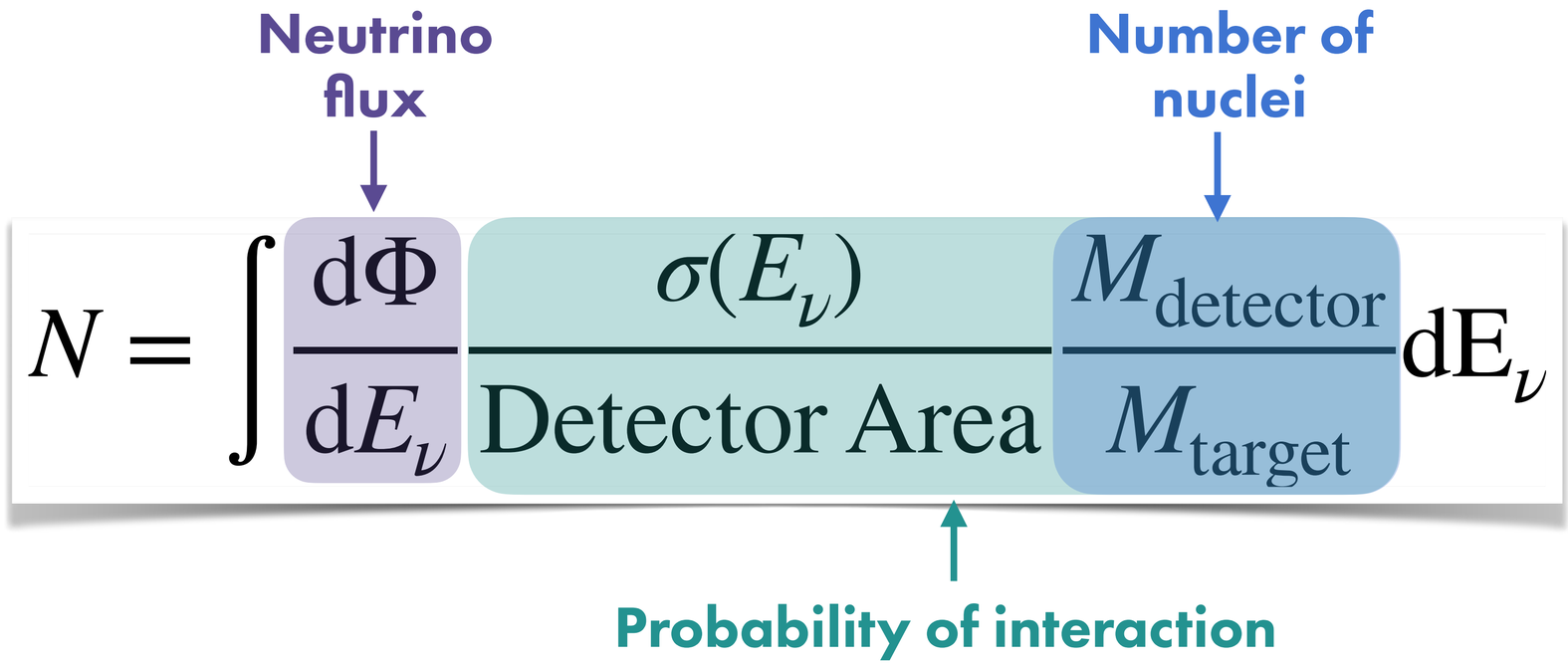
Neutrino flux
Number of nuclei
$N = \int \frac{d\Phi}{dE_\nu} \frac{\sigma(E_\nu)}{\text{Detector Area}} \frac{M_{\text{detector}}}{M_{\text{target}}} dE_\nu$
Probability of interaction

Fluxes

Fluxes

[Laura Fields - DUNE fluxes]

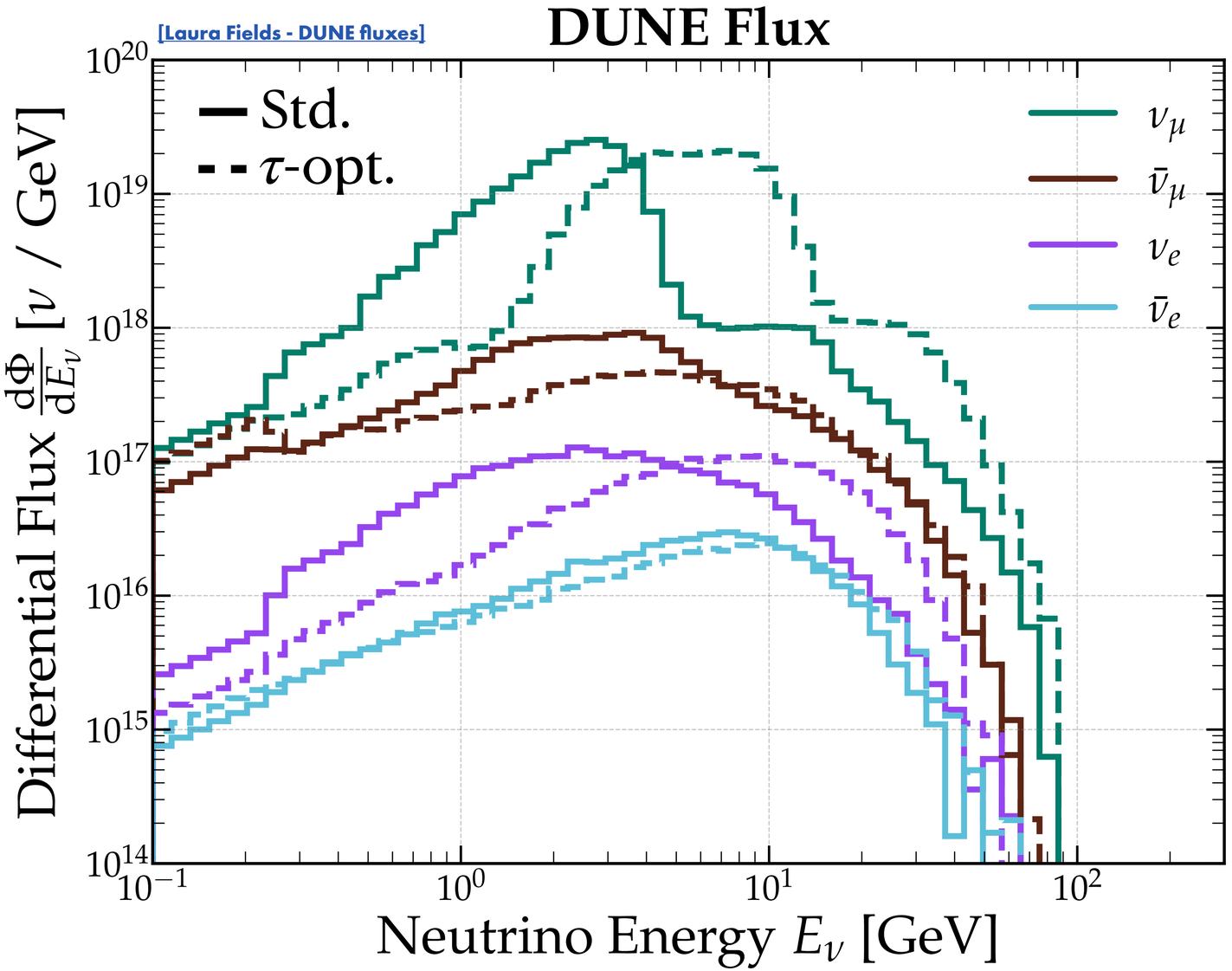

Fluxes

[Laura Fields - DUNE fluxes]

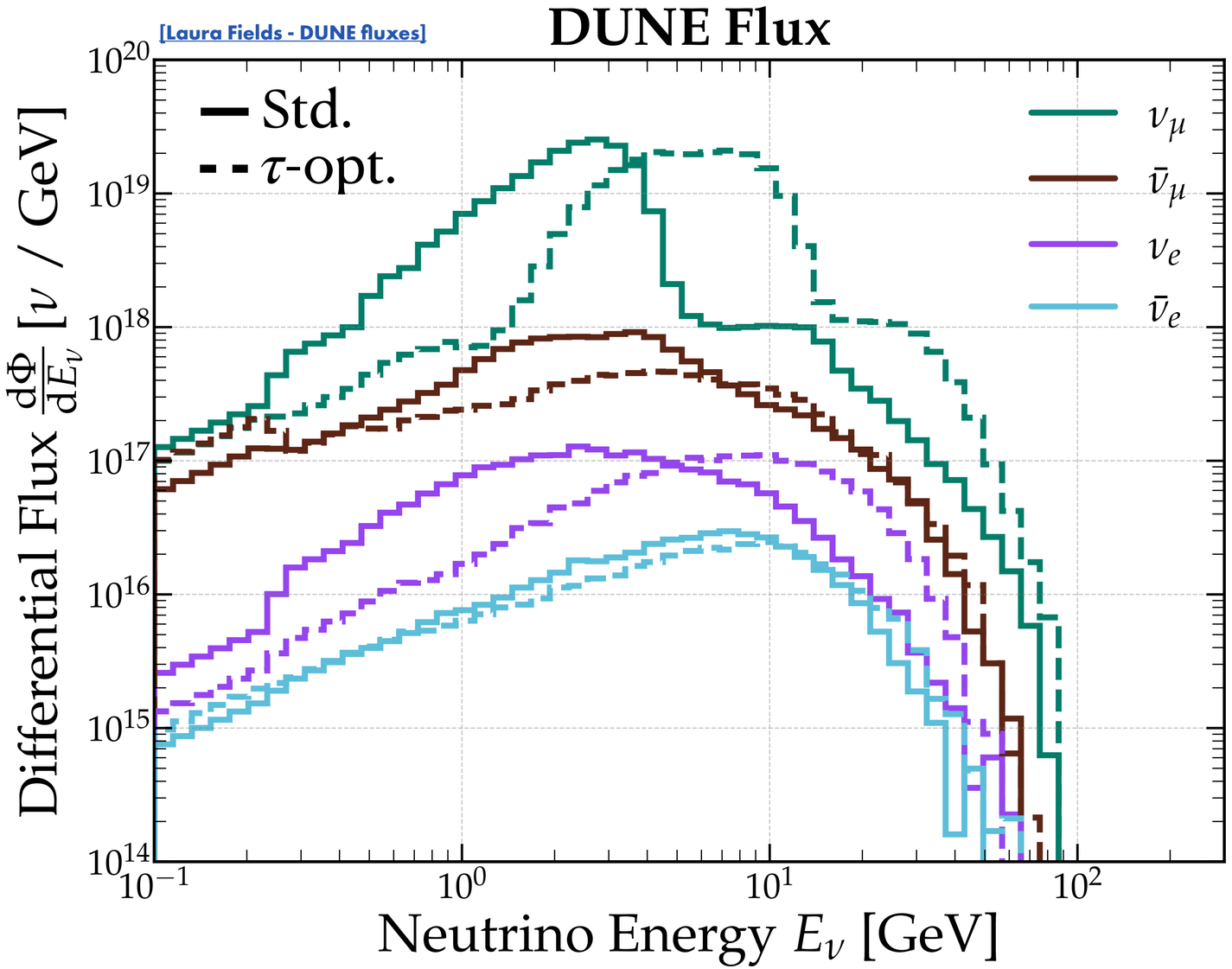

Standard CP-optimized Flux

- ν's mostly in the $1 - 5$ GeV range.
- Peak at ~ 2 GeV.
- Better for δ_{CP} measurements.

Fluxes

[Laura Fields - DUNE fluxes]

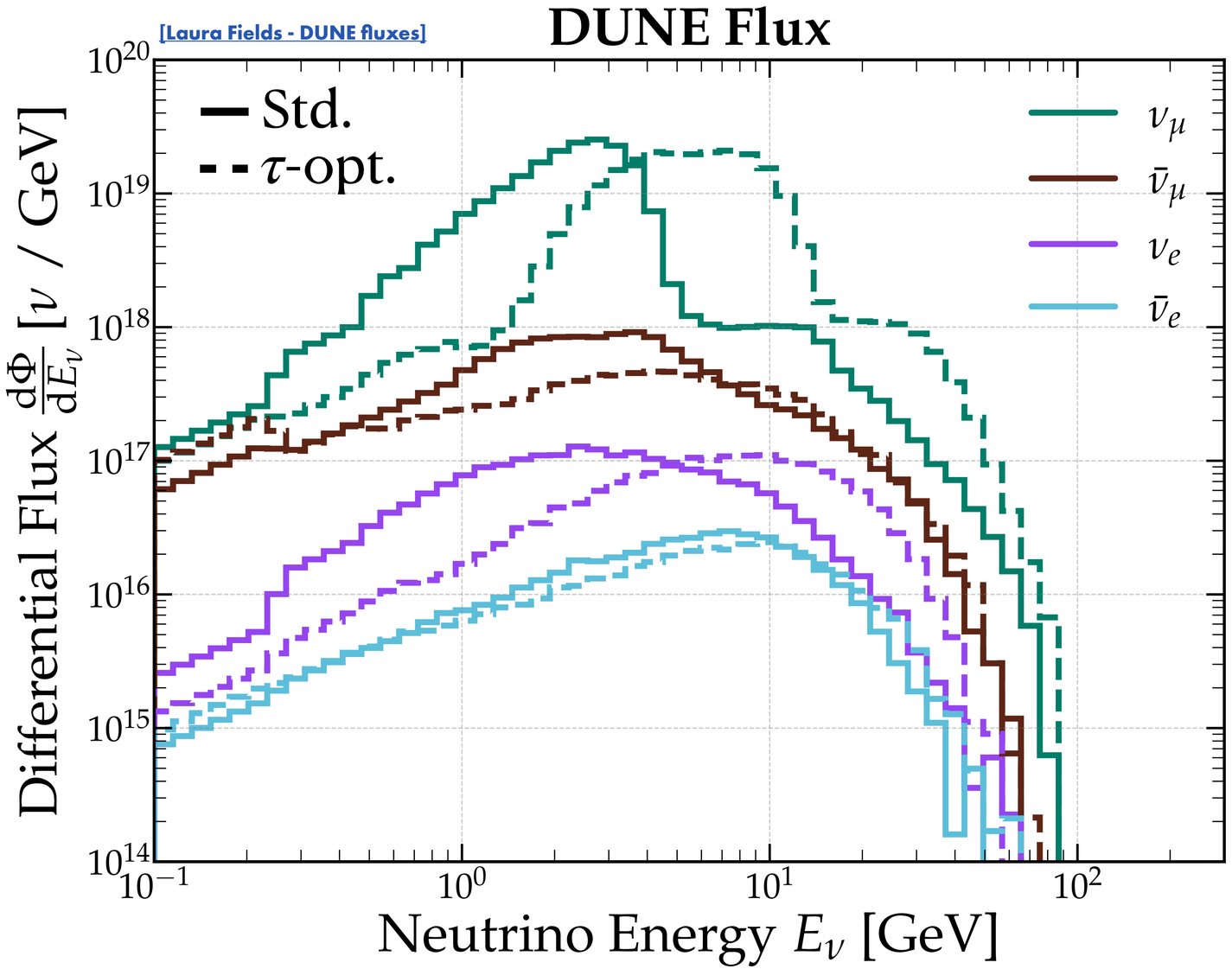

Standard CP-optimized Flux

- ν's mostly in the $1 - 5$ GeV range.
- Peak at ~ 2 GeV.
- Better for δ_{CP} measurements.

Tau-optimized Flux

- Higher energy ν flux.
- Peak at ~ 4 GeV.
- Better for ν_τ measurements.

Fluxes

[Laura Fields - DUNE fluxes]

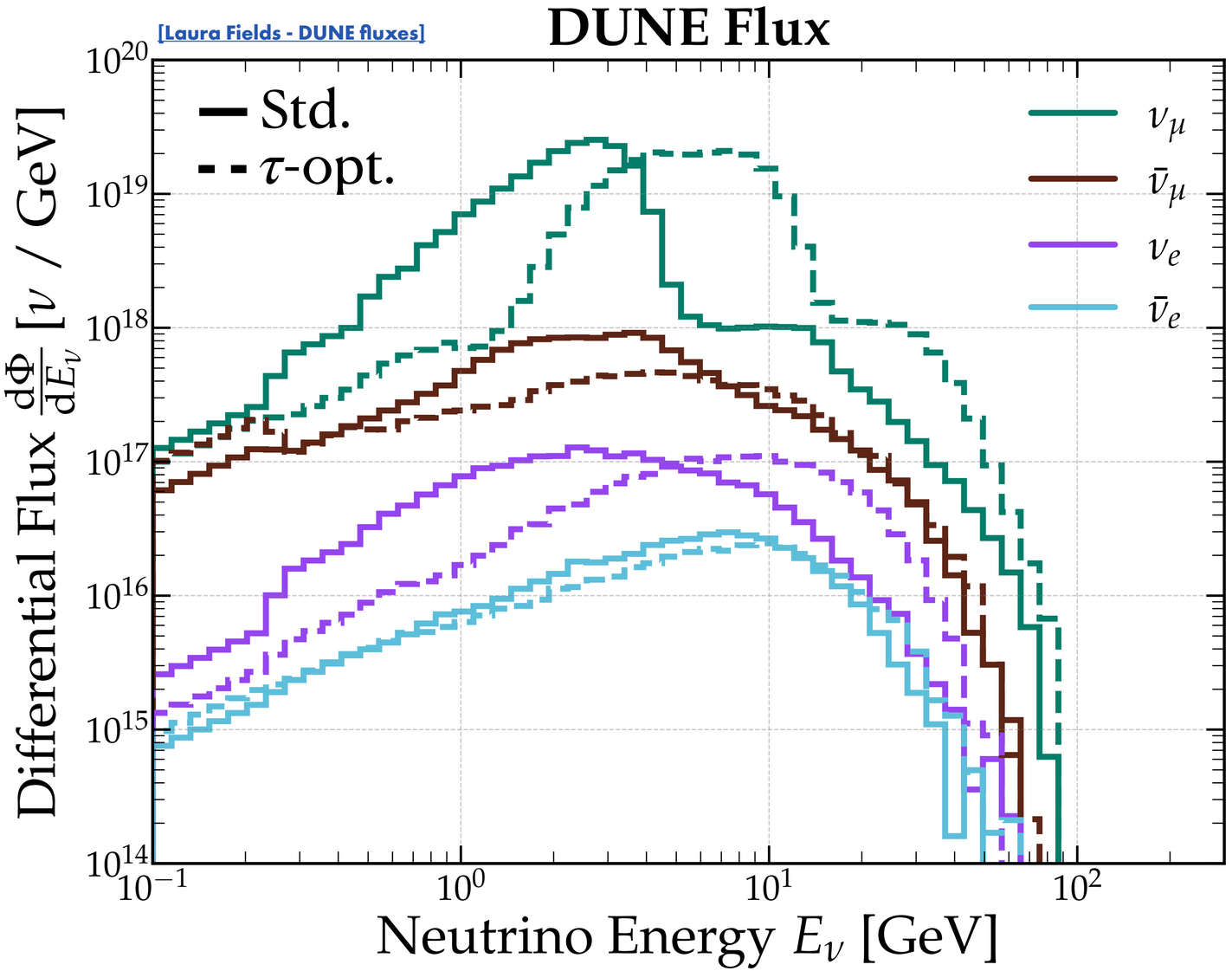

Standard CP-optimized Flux

- ν's mostly in the $1 - 5$ GeV range.
- Peak at ~ 2 GeV.
- Better for δ_{CP} measurements.

Tau-optimized Flux

- Higher energy ν flux.
- Peak at ~ 4 GeV.
- Better for ν_τ measurements.

Exposure: 3.3×10^{21} POT

Detector Area: $5\,\mathrm{m} \times 3\,\mathrm{m}$

Detector Mass: 67 tonnes of $^{40}_{18}\mathrm{Ar}$

DUNE Standard Flux ν-mode

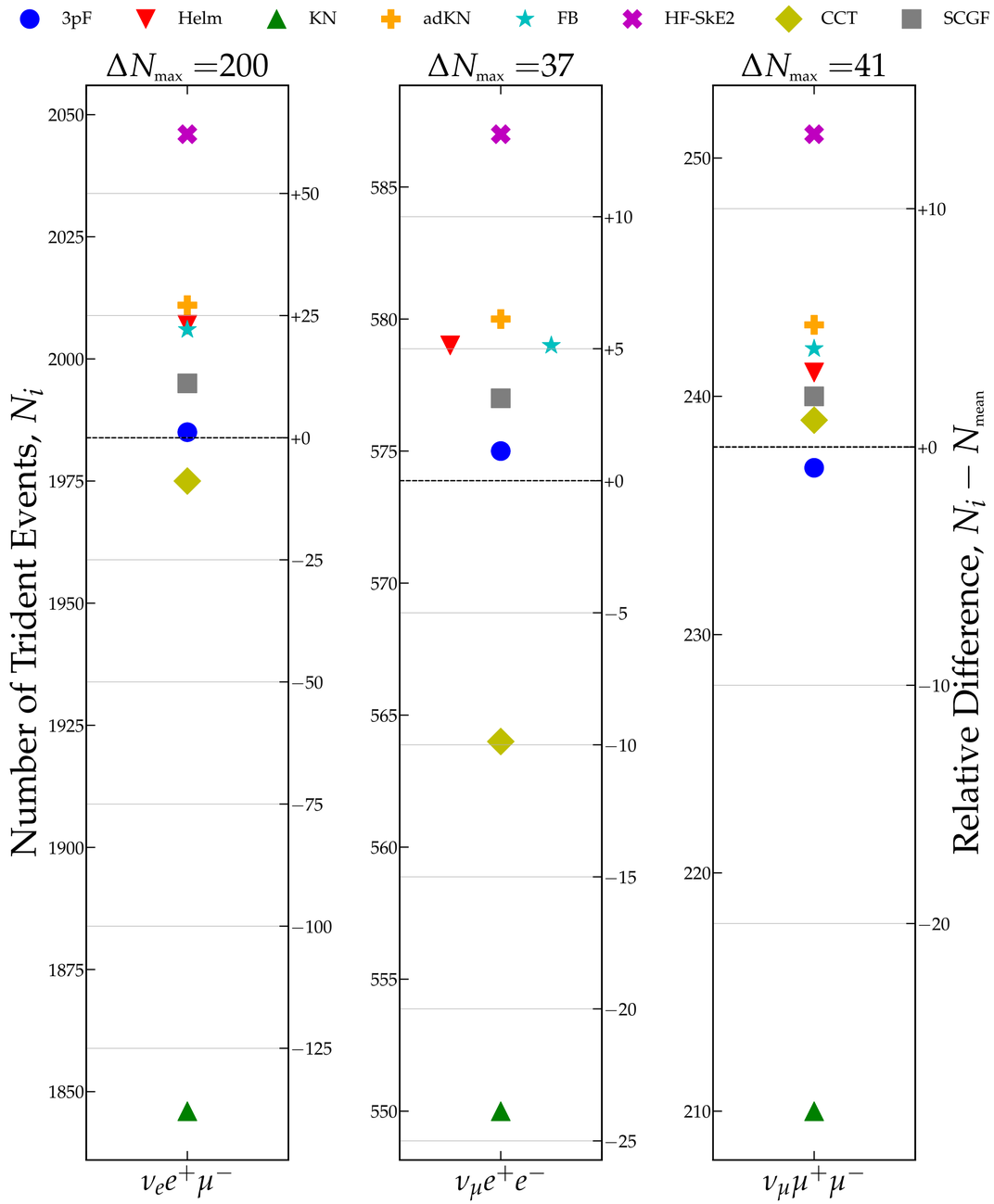

DUNE Tau-optimized Flux ν-mode

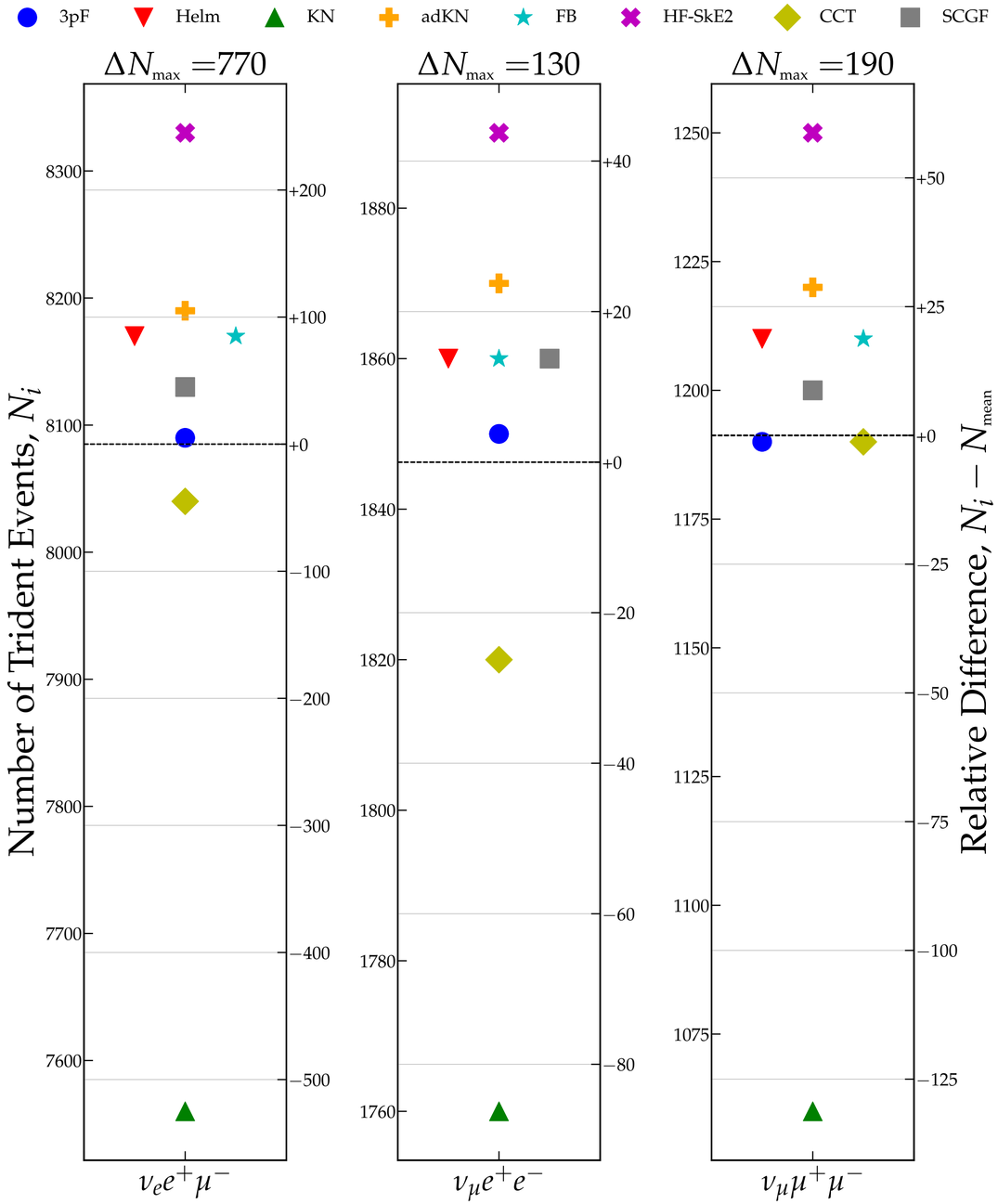

Fluxes

[Provided by Vishvas Pandey]

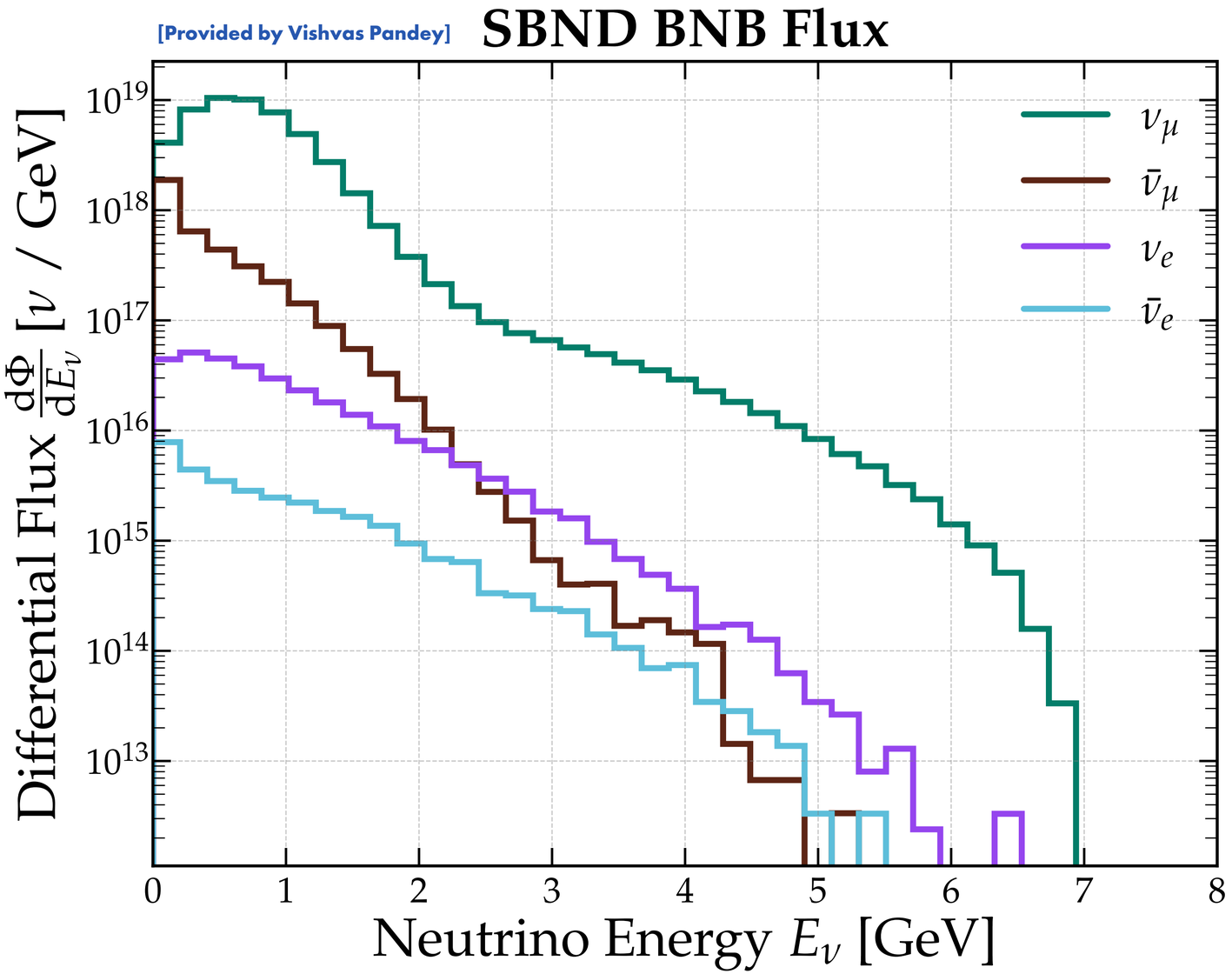

Fluxes

[Provided by Vishvas Pandey]

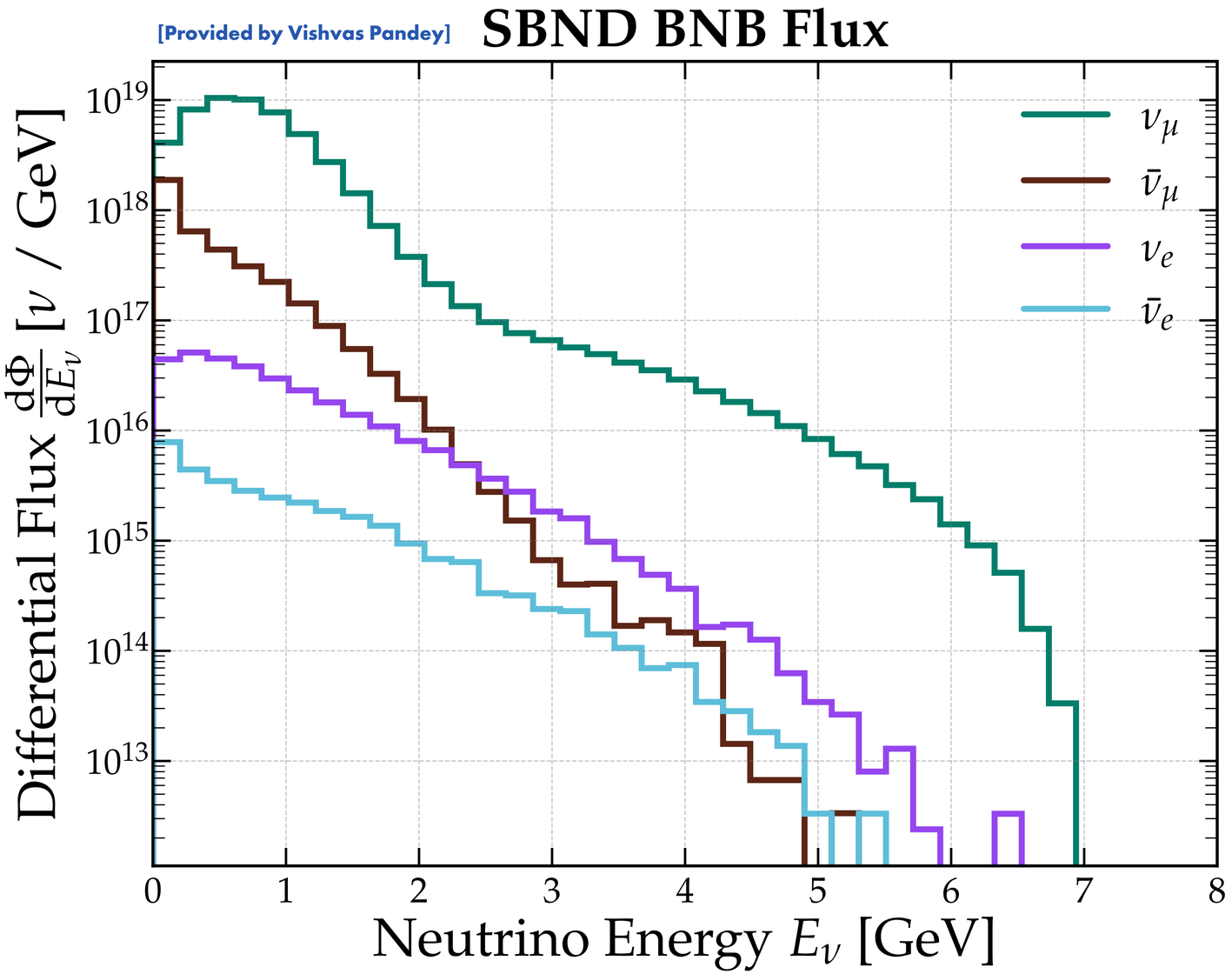

- Flux from on-axis BNB beam at Fermilab
- ν's mostly in the $\lesssim 3$ GeV range
- Peak at ~ 500 MeV

Fluxes

[Provided by Vishvas Pandey]

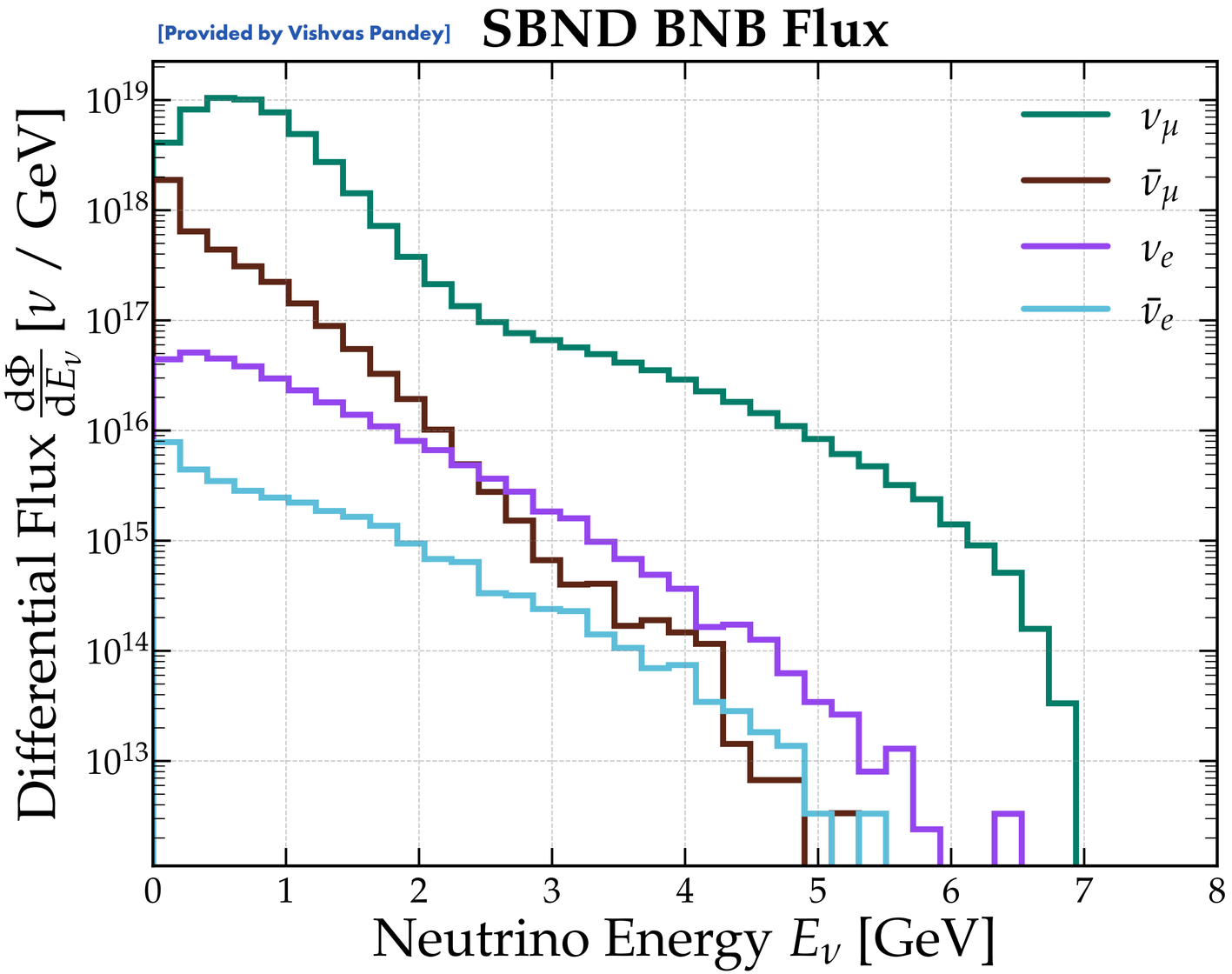

- Flux from on-axis BNB beam at Fermilab
- ν's mostly in the $\lesssim 3$ GeV range
- Peak at ~ 500 MeV

Exposure: 1×10^{21} POT

Detector Area: $4\,\mathrm{m} \times 4\,\mathrm{m}$

Detector Mass: 112 tonnes of $^{40}_{18}\mathrm{Ar}$

Fluxes

[2504.08950]

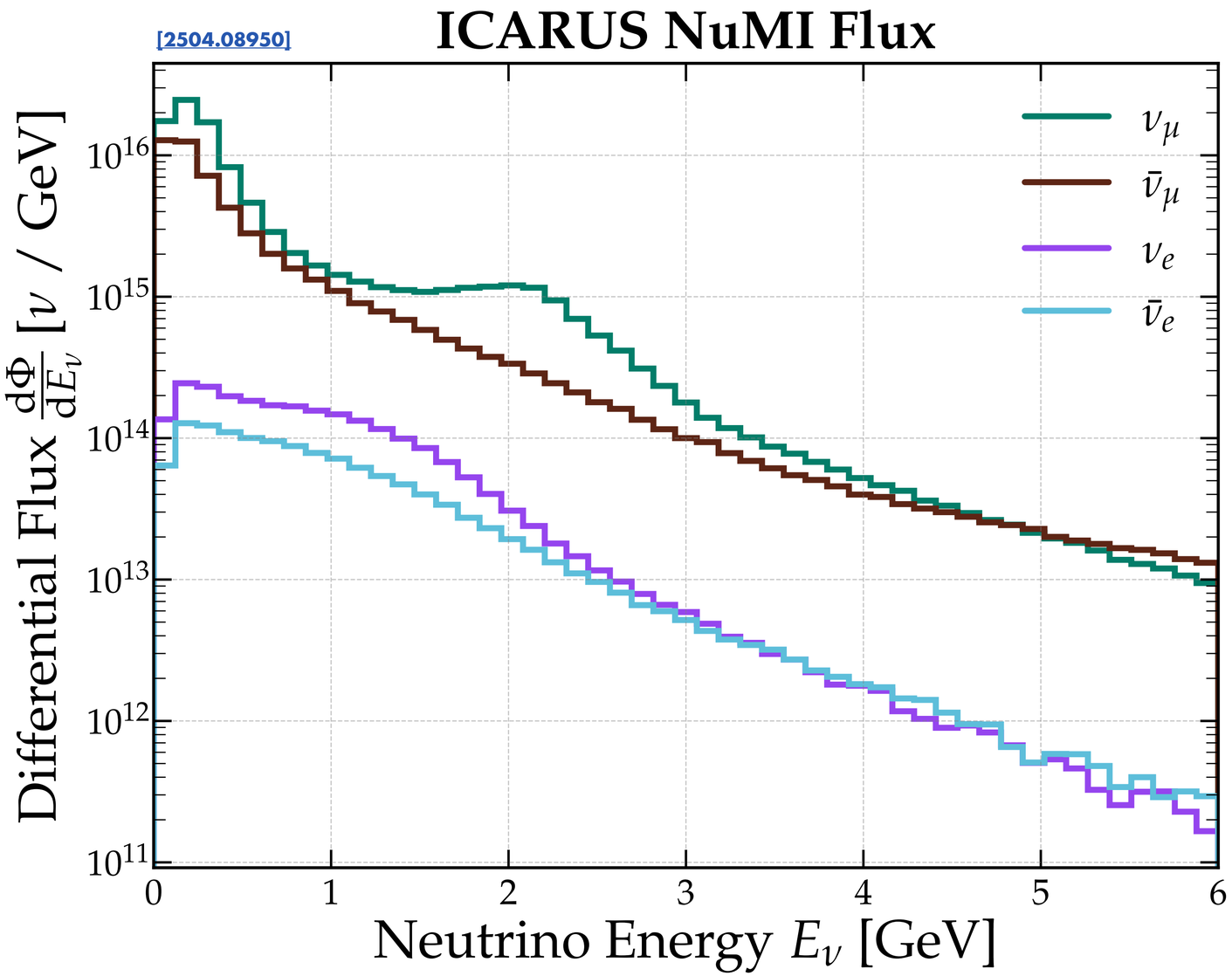

Fluxes

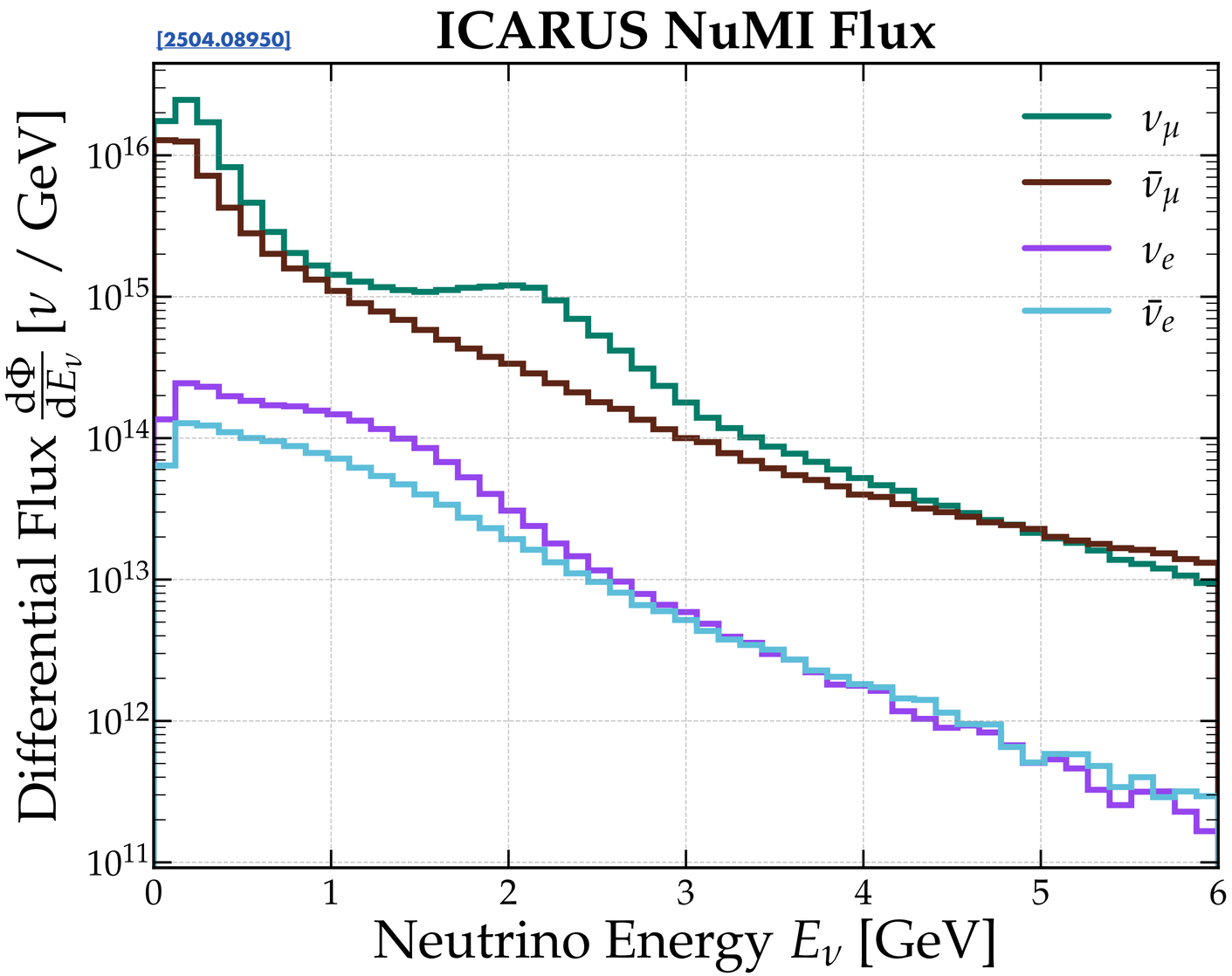

- Flux from off-axis NuMI beam at Fermilab
- ν's mostly in the $\lesssim 3$ GeV range
- Peak at ~ 200 MeV

Fluxes

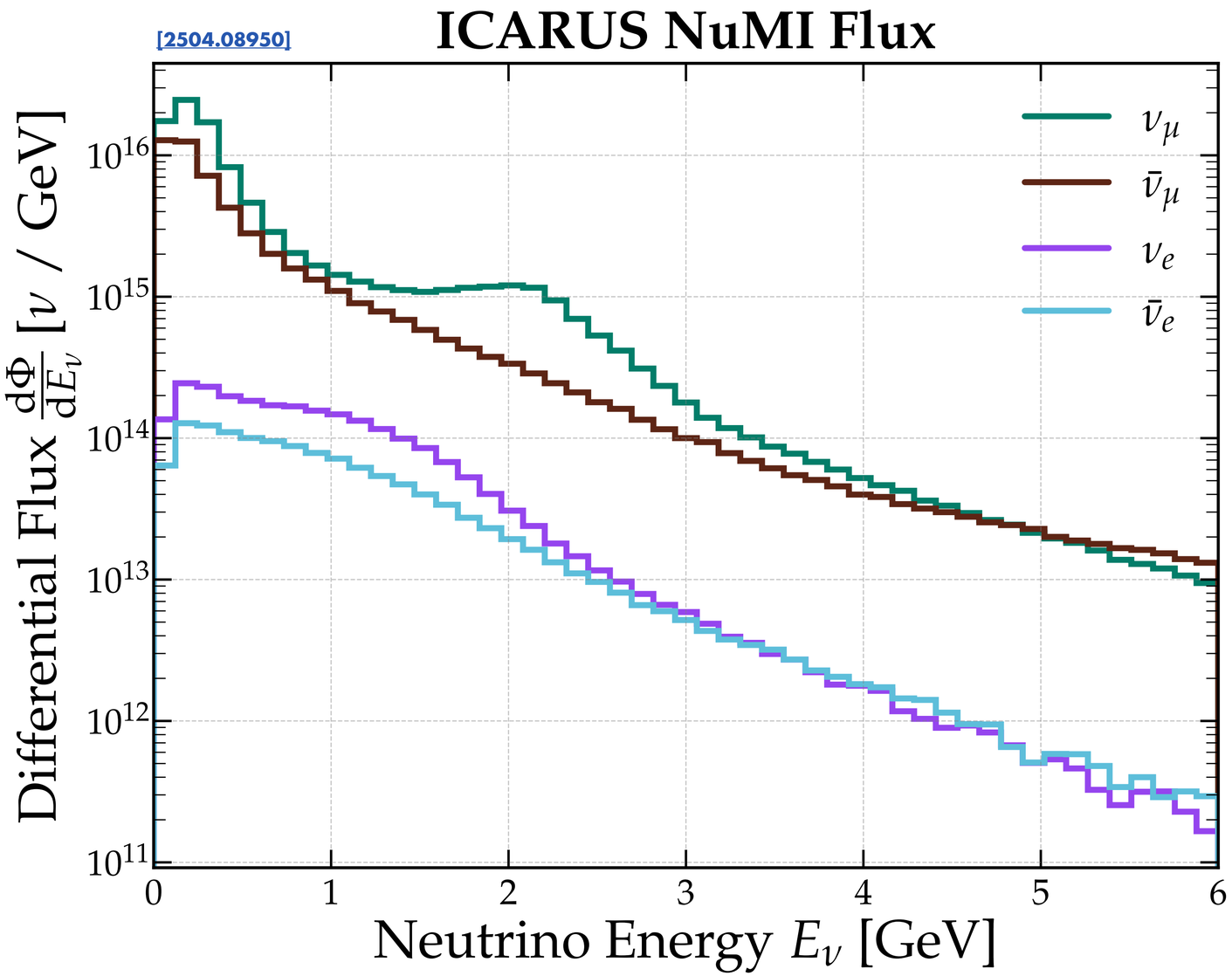

- Flux from off-axis NuMI beam at Fermilab
- ν's mostly in the $\lesssim 3$ GeV range
- Peak at ~ 200 MeV

Exposure: 1.8×10^{21} POT

Detector Area: $3.6\,\mathrm{m} \times 3.9\,\mathrm{m}$

Detector Mass: 476 tonnes of $^{40}_{18}\mathrm{Ar}$

SBND BNB Flux ν-mode

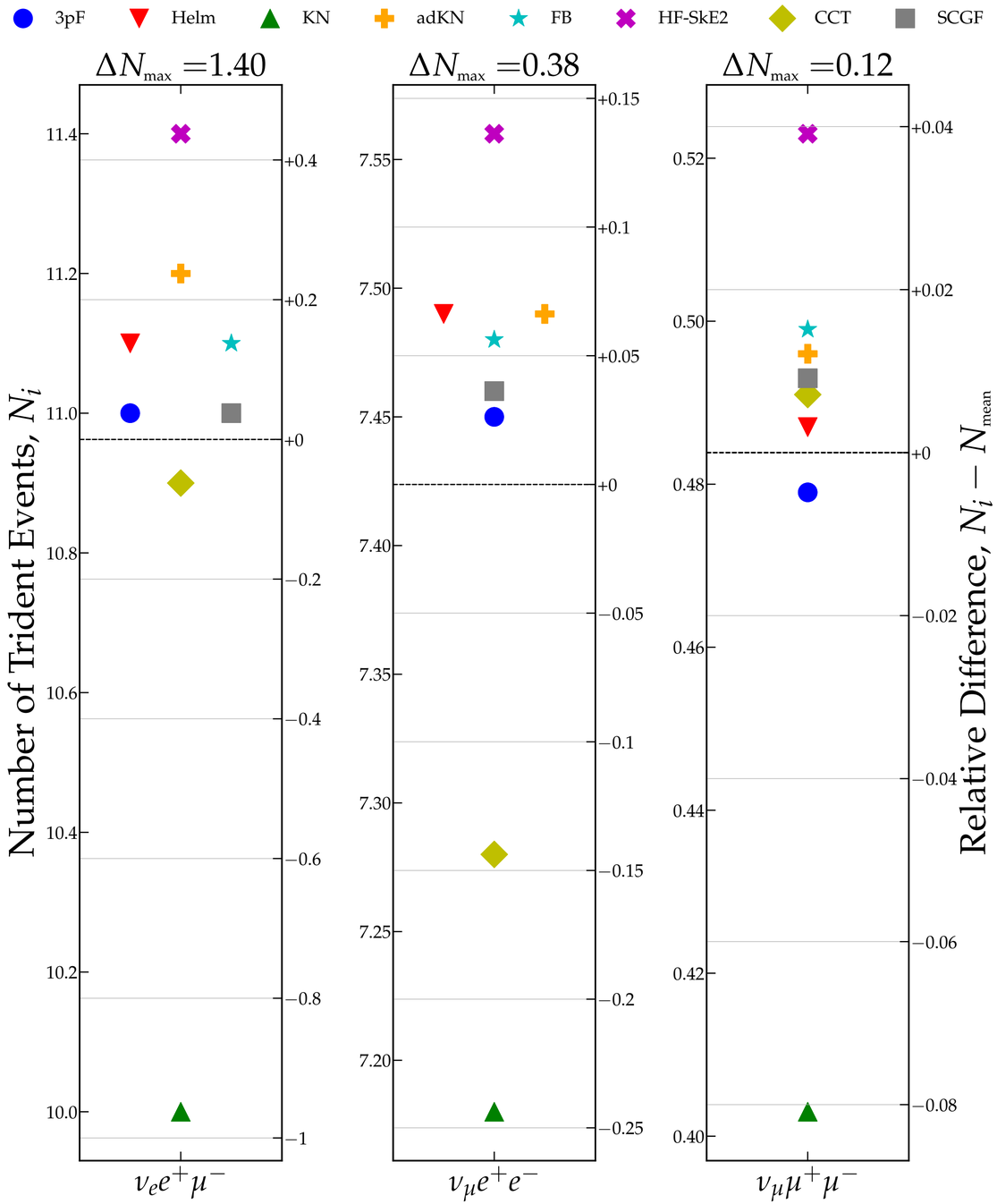

ICARUS NuMI Flux ν-mode

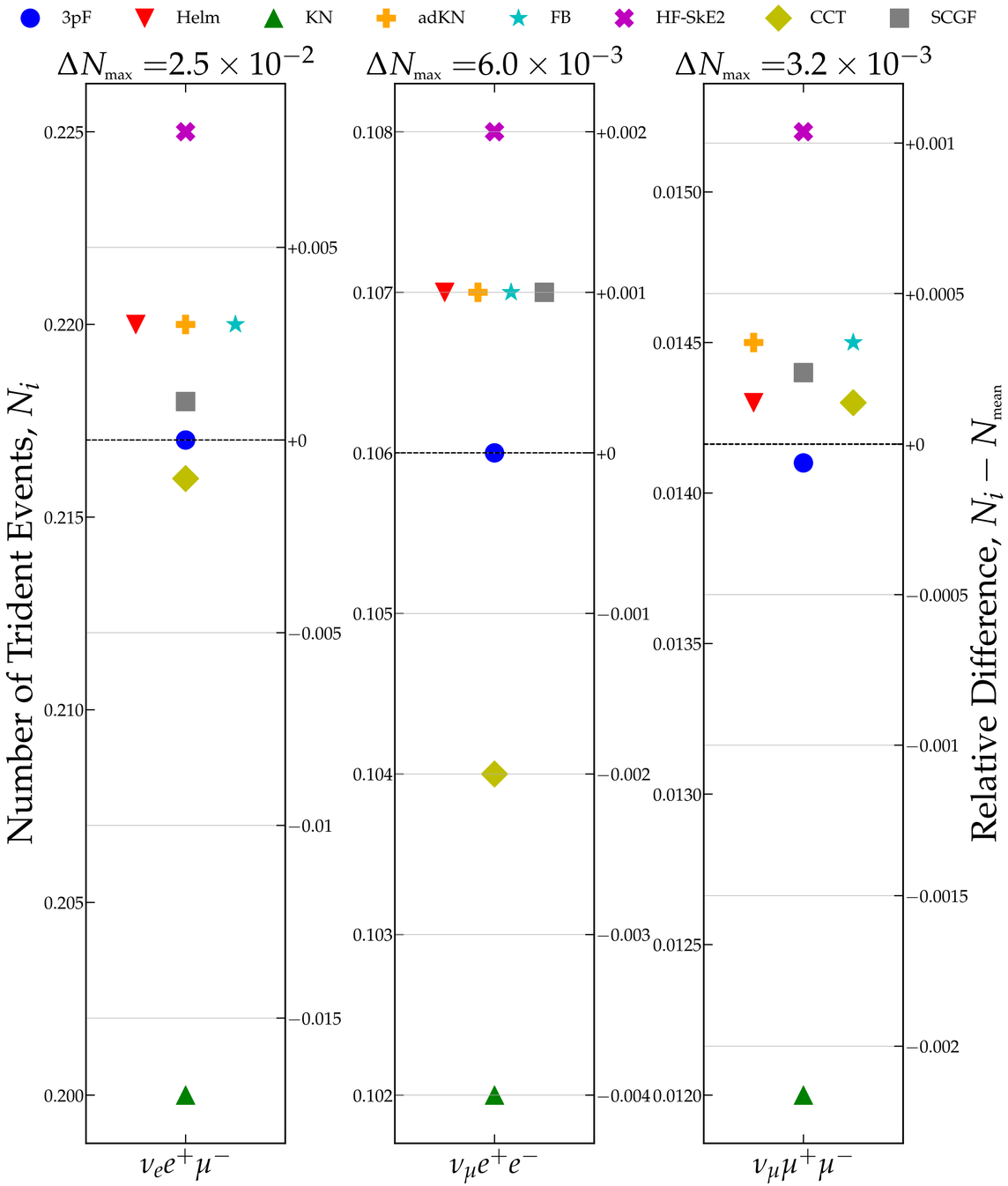

Fluxes

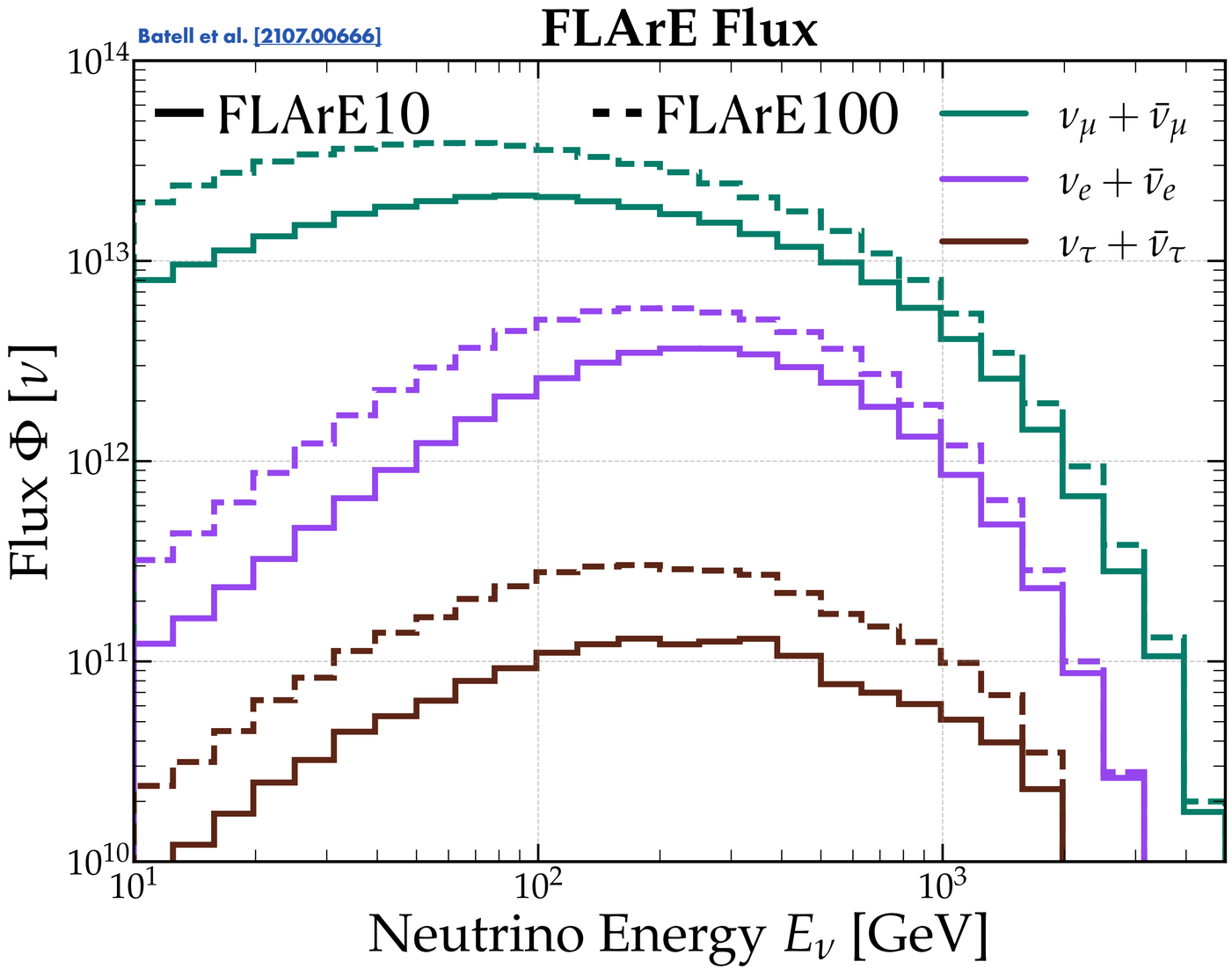
Batell et al. [2107.00666]
FLArE Flux
FLArE10
FLArE100
$\nu_\mu + \bar{\nu}_\mu$
$\nu_e + \bar{\nu}_e$
$\nu_\tau + \bar{\nu}_\tau$
Flux Φ [ν]
10^{14}
10^{13}
10^{12}
10^{11}
10^{10}
10^1
10^2
10^3
Neutrino Energy E_ν [GeV]

Fluxes

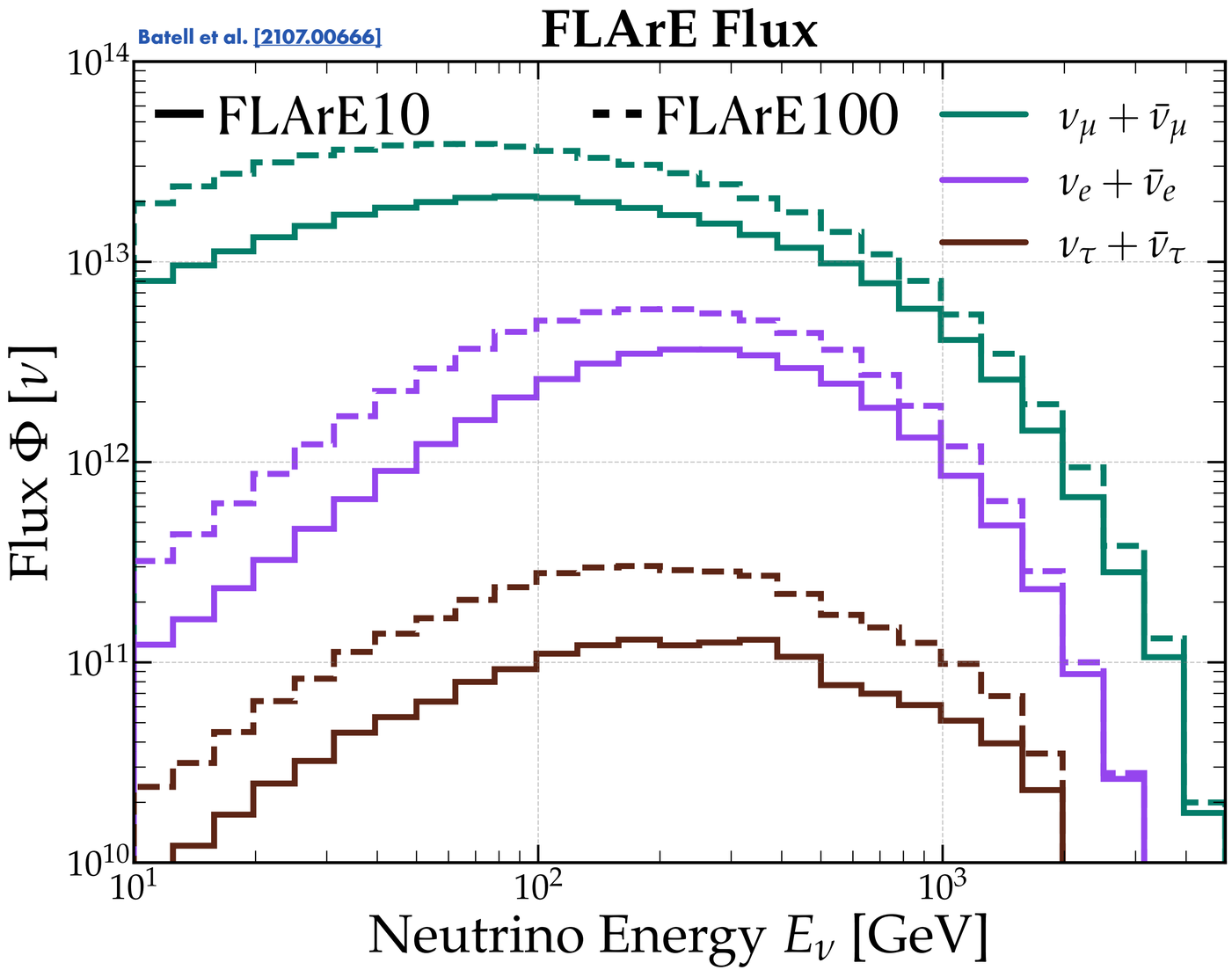

- Located 620 m from the ATLAS IP
- Generated with the SYBILL 2.3c event generator and the fast neutrino flux simulation Kling & Nevay [2105.08270]

Fluxes

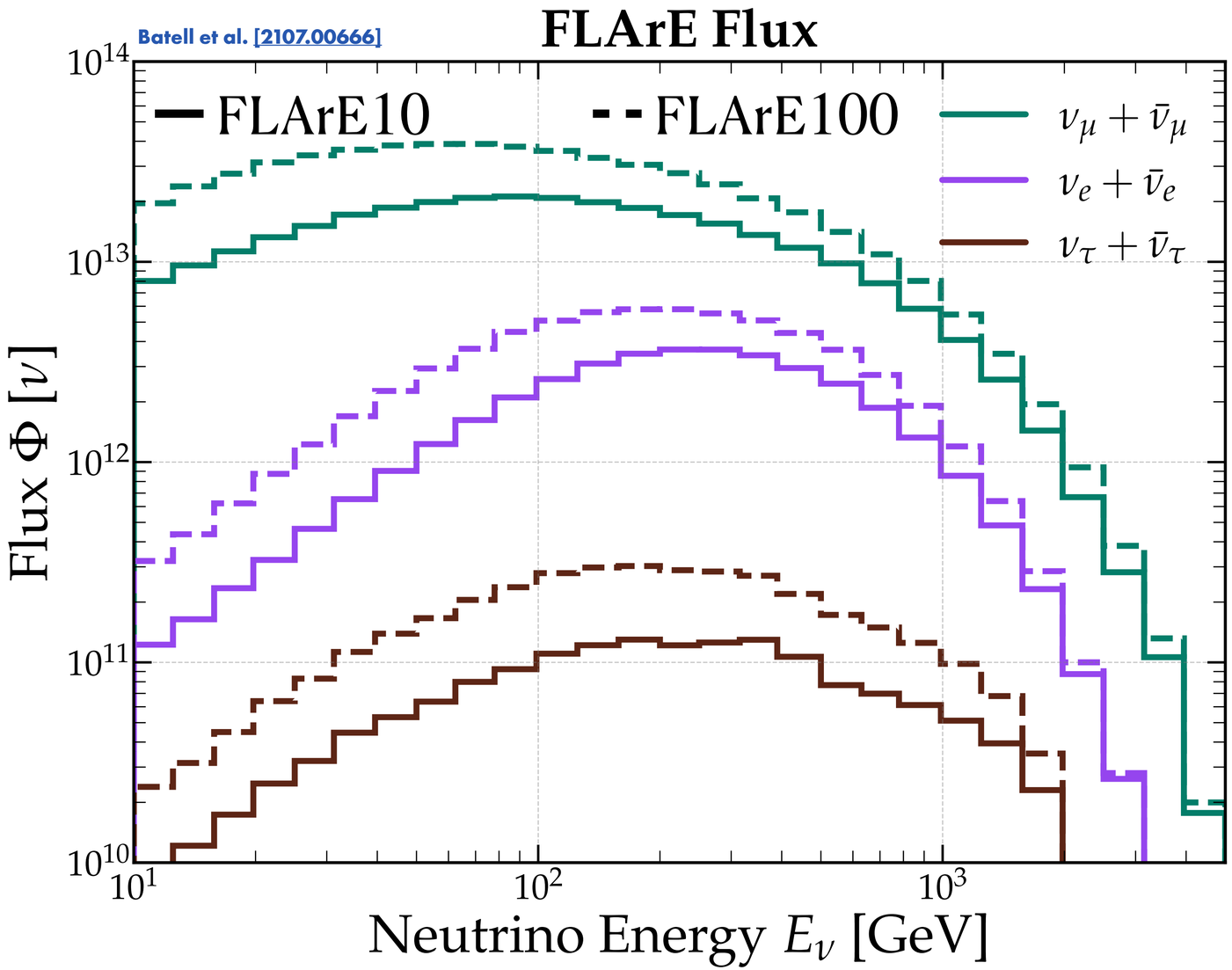

- Located 620 m from the ATLAS IP
- Generated with the SYBILL 2.3c event generator and the fast neutrino flux simulation Kling & Nevay [2105.08270]

Luminosity: $3000\ \mathrm{fb}^{-1}$

FLArE10

Detector Area: $1\ \mathrm{m} \times 1\ \mathrm{m}$

Detector Mass: 10 tonnes of $^{40}_{18}\mathrm{Ar}$

Fluxes

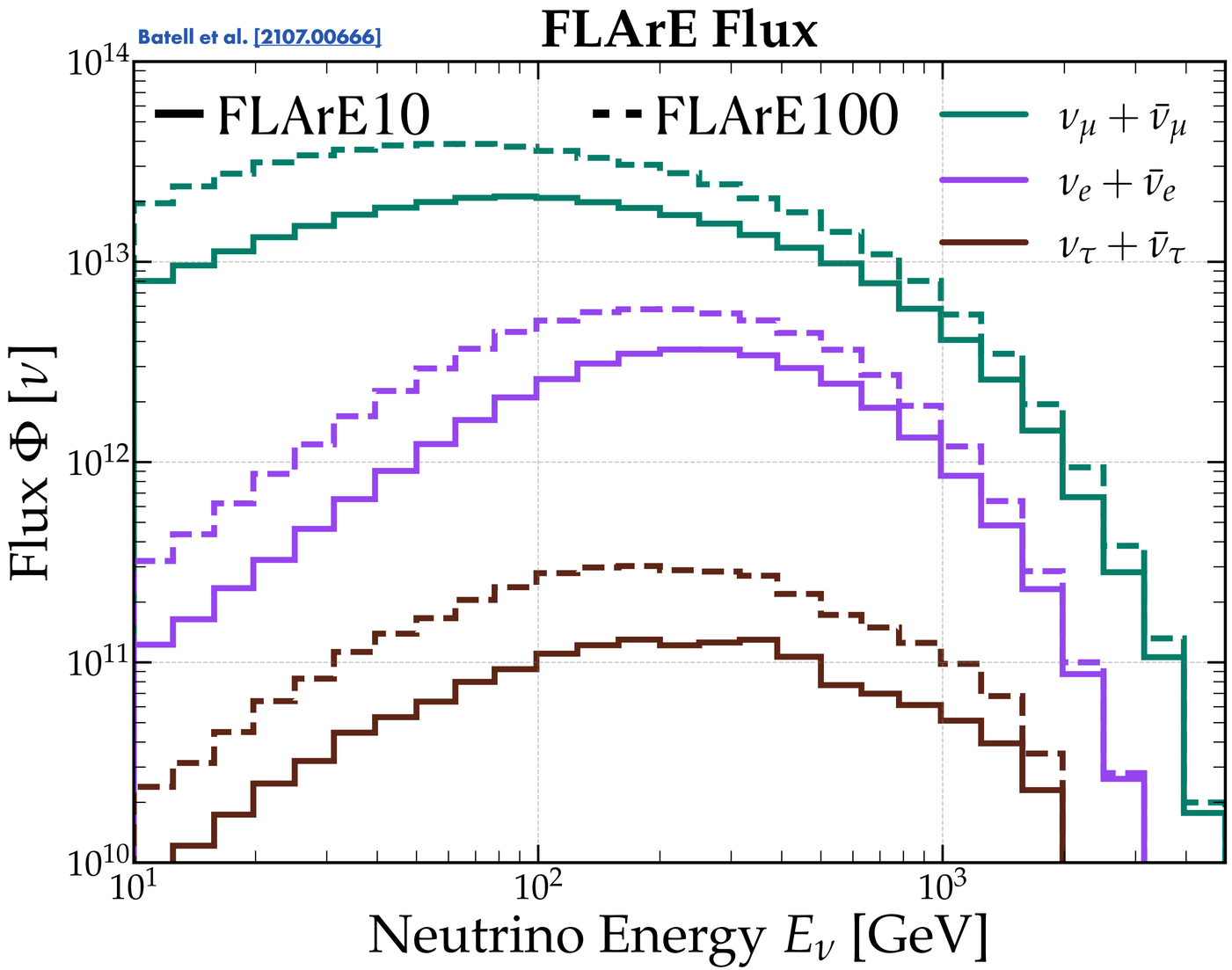

- Located 620 m from the ATLAS IP
- Generated with the SYBILL 2.3c event generator and the fast neutrino flux simulation Kling & Nevay [2105.08270]

Luminosity: $3000\ \mathrm{fb}^{-1}$

FLArE10

Detector Area: $1\ \mathrm{m} \times 1\ \mathrm{m}$

Detector Mass: 10 tonnes of $^{40}_{18}\mathrm{Ar}$

FLArE100

Detector Area: $1.6\ \mathrm{m} \times 1.6\ \mathrm{m}$

Detector Mass: 100 tonnes of $^{40}_{18}\mathrm{Ar}$

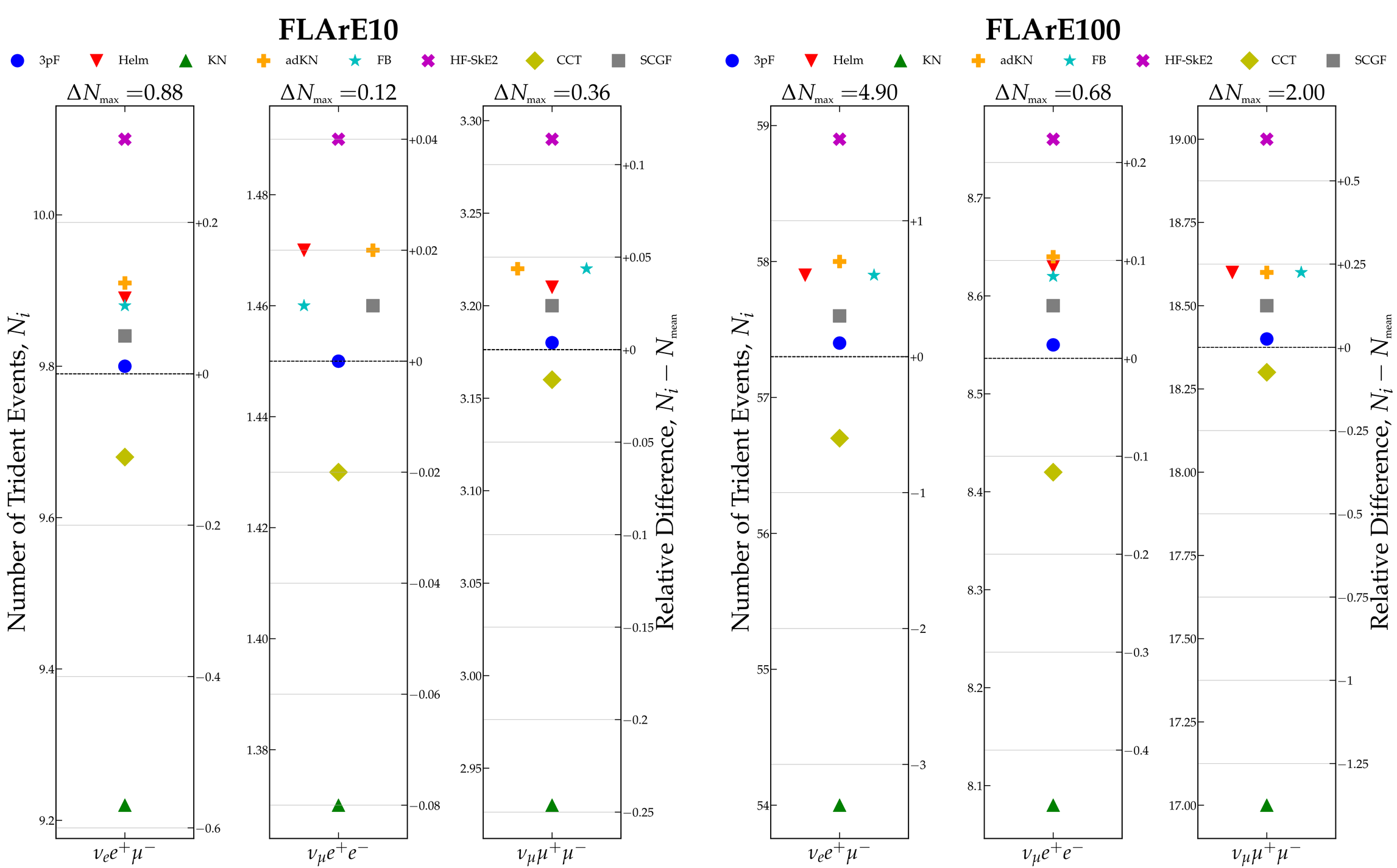
FLArE10
FLArE100
3pF
Helm
KN
adKN
FB
HF-SkE2
CCT
SCGF
$\Delta N_{\max}$ =0.88
$\Delta N_{\max}$ =0.12
$\Delta N_{\max}$ =0.36
$\Delta N_{\max}$ =4.90
$\Delta N_{\max}$ =0.68
$\Delta N_{\max}$ =2.00
Number of Trident Events, N_i
Relative Difference, $N_i - N_{\text{mean}}$
$\nu_e e^+ \mu^-$
$\nu_\mu e^+ e^-$
$\nu_\mu \mu^+ \mu^-$

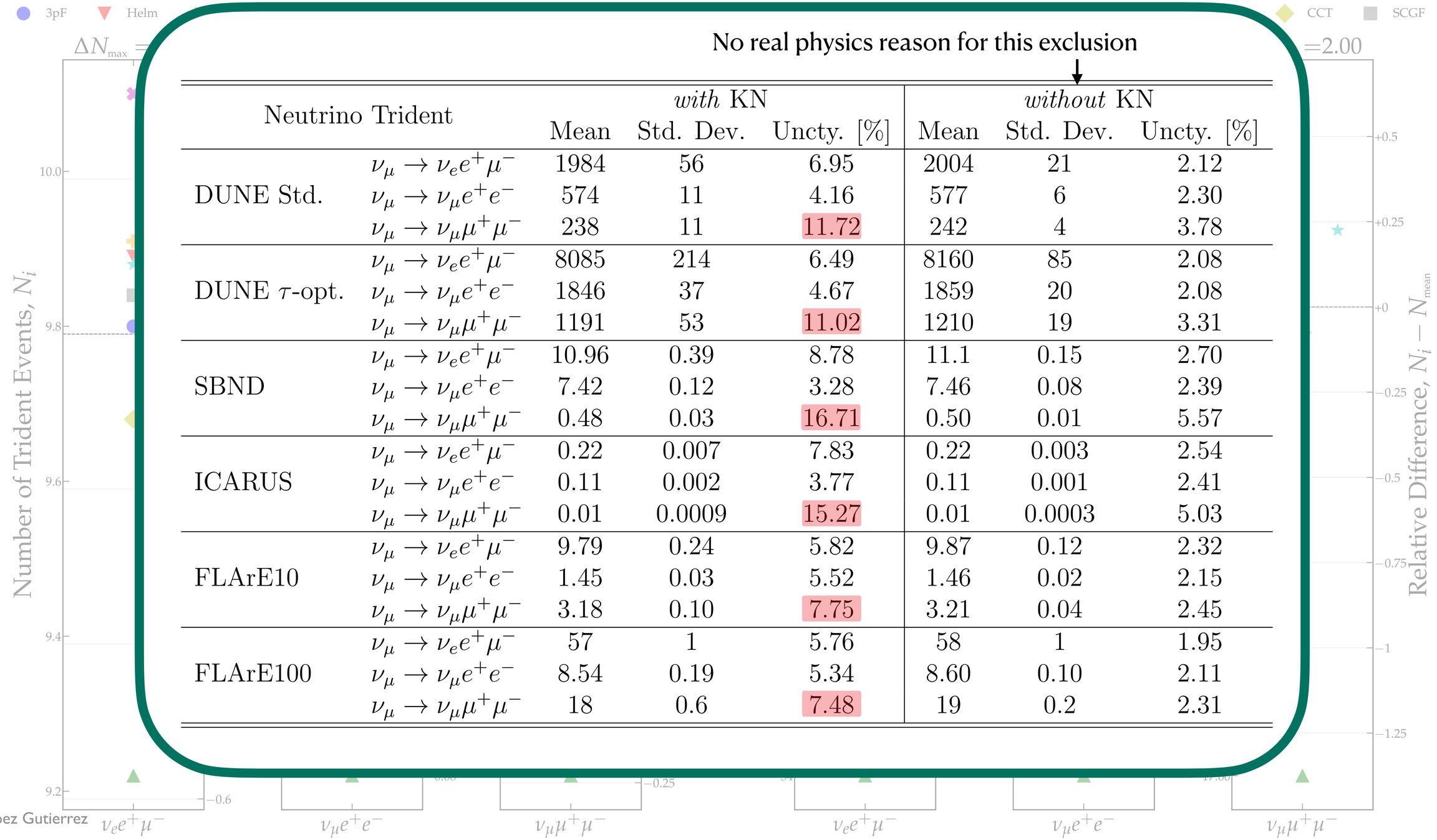

No real physics reason for this exclusion

Neutrino Trident		*with* KN			*without* KN		
		Mean	Std. Dev.	Uncty. [%]	Mean	Std. Dev.	Uncty. [%]
DUNE Std.	$\nu_\mu \to \nu_e e^+\mu^-$	1984	56	6.95	2004	21	2.12
	$\nu_\mu \to \nu_\mu e^+e^-$	574	11	4.16	577	6	2.30
	$\nu_\mu \to \nu_\mu \mu^+\mu^-$	238	11	11.72	242	4	3.78
DUNE τ-opt.	$\nu_\mu \to \nu_e e^+\mu^-$	8085	214	6.49	8160	85	2.08
	$\nu_\mu \to \nu_\mu e^+e^-$	1846	37	4.67	1859	20	2.08
	$\nu_\mu \to \nu_\mu \mu^+\mu^-$	1191	53	11.02	1210	19	3.31
SBND	$\nu_\mu \to \nu_e e^+\mu^-$	10.96	0.39	8.78	11.1	0.15	2.70
	$\nu_\mu \to \nu_\mu e^+e^-$	7.42	0.12	3.28	7.46	0.08	2.39
	$\nu_\mu \to \nu_\mu \mu^+\mu^-$	0.48	0.03	16.71	0.50	0.01	5.57
ICARUS	$\nu_\mu \to \nu_e e^+\mu^-$	0.22	0.007	7.83	0.22	0.003	2.54
	$\nu_\mu \to \nu_\mu e^+e^-$	0.11	0.002	3.77	0.11	0.001	2.41
	$\nu_\mu \to \nu_\mu \mu^+\mu^-$	0.01	0.0009	15.27	0.01	0.0003	5.03
FLArE10	$\nu_\mu \to \nu_e e^+\mu^-$	9.79	0.24	5.82	9.87	0.12	2.32
	$\nu_\mu \to \nu_\mu e^+e^-$	1.45	0.03	5.52	1.46	0.02	2.15
	$\nu_\mu \to \nu_\mu \mu^+\mu^-$	3.18	0.10	7.75	3.21	0.04	2.45
FLArE100	$\nu_\mu \to \nu_e e^+\mu^-$	57	1	5.76	58	1	1.95
	$\nu_\mu \to \nu_\mu e^+e^-$	8.54	0.19	5.34	8.60	0.10	2.11
	$\nu_\mu \to \nu_\mu \mu^+\mu^-$	18	0.6	7.48	19	0.2	2.31

Summary

Summary

- **Precision SM analysis and BSM searches using neutrino tridents feasible** for the first time thanks to current and next-generation neutrino experiments!

Summary

- **Precision SM analysis and BSM searches using neutrino tridents feasible** for the first time thanks to current and next-generation neutrino experiments!
- Coherent neutrino trident scattering is the dominant channel and requires **accurate SM event rates for proper comparison to BSM predictions**. Neutrino trident event rate **uncertainty mostly coming from nuclear physics**; focus on argon nuclear form factor.
  - Previously underestimated uncertainty of $\sim 1\,\%$
  - No experimental data since 1982 and the available data is constrained to small momentum transfer range
  - Calculated cross sections and event rates using multiple popular form factor parameterizations and found uncertainties as high as $11\,\%$ and $\Delta N = 770$ for $\nu_\mu \to \nu_e e^+ \mu^-$ with the DUNE τ-optimized flux.

Summary

- **Precision SM analysis and BSM searches using neutrino tridents feasible** for the first time thanks to current and next-generation neutrino experiments!
- Coherent neutrino trident scattering is the dominant channel and requires **accurate SM event rates for proper comparison to BSM predictions**. Neutrino trident event rate **uncertainty mostly coming from nuclear physics**; focus on argon nuclear form factor.
  - Previously underestimated uncertainty of $\sim 1\,\%$
  - No experimental data since 1982 and the available data is constrained to small momentum transfer range
  - Calculated cross sections and event rates using multiple popular form factor parameterizations and found uncertainties as high as $11\,\%$ and $\Delta N = 770$ for $\nu_\mu \to \nu_e e^+ \mu^-$ with the DUNE τ-optimized flux.
- **New argon electric form factor measurements spanning a wider range of momentum transfer** are imperative to fully explore the physics potential of current and next-generation neutrino experiments!

Summary

- **Precision SM analysis and BSM searches using neutrino tridents feasible** for the first time thanks to current and next-generation neutrino experiments!
- Coherent neutrino trident scattering is the dominant channel and requires **accurate SM event rates for proper comparison to BSM predictions**. Neutrino trident event rate **uncertainty mostly coming from nuclear physics**; focus on argon nuclear form factor.
  - Previously underestimated uncertainty of $\sim 1\,\%$
  - No experimental data since 1982 and the available data is constrained to small momentum transfer range
  - Calculated cross sections and event rates using multiple popular form factor parameterizations and found uncertainties as high as $11\,\%$ and $\Delta N = 770$ for $\nu_\mu \to \nu_e e^+ \mu^-$ with the DUNE τ-optimized flux.
- **New argon electric form factor measurements spanning a wider range of momentum transfer** are imperative to fully explore the physics potential of current and next-generation neutrino experiments!

Thank you!

Back-up Slides

Argon Charged Form Factor

- Woods-Saxon 3-parameter Fermi: Fourier transform of the spherically symmetric nuclear charge density distribution $\rho_N(r)$ with

$$\rho_N(r) = \mathcal{N}\frac{1+\frac{wr^2}{c^2}}{1+\exp(\frac{r-c}{z})},$$

and

$$F_{\mathrm{WS}}(Q^2) = \int \mathrm{d}r r^2 j_0(Qr)\rho_N(r)\,.$$

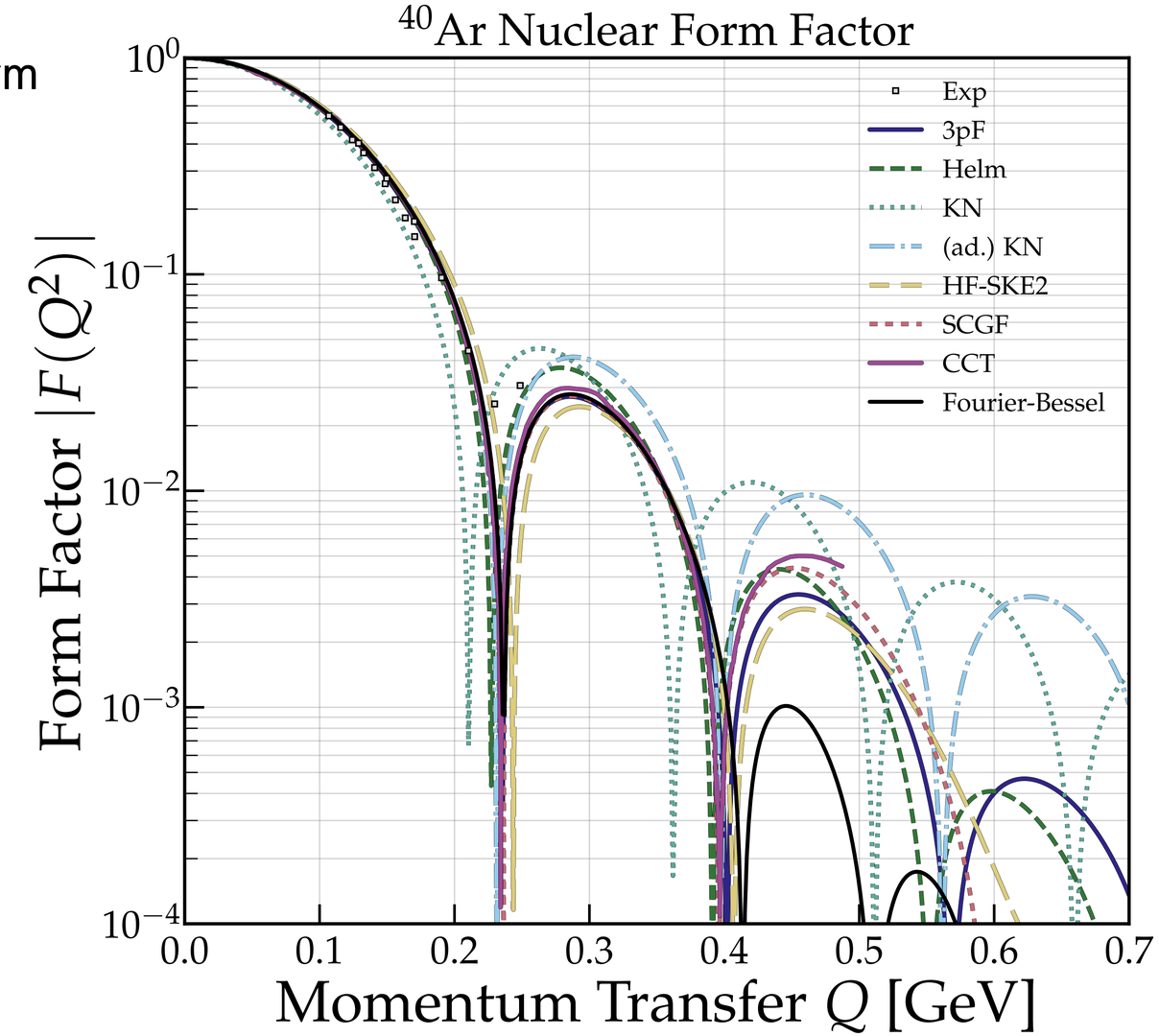

Argon Charged Form Factor

- Woods-Saxon 3-parameter Fermi
  De Vries et al. [Atom. Data Nucl. Data Tabl. 1987]
- Helm: nuclear charge density distribution is described as a convolution of a uniform density ρ_0 with radius R_0 and a Gaussian profile ρ_1 characterized by a folding width s, which accounts for the nuclear surface thickness. The form factor is given by

$$F_{\mathrm{H}}(Q^2) = \frac{3j_1(QR_0)}{QR_0} e^{-\frac{Q^2 s^2}{2}} .$$

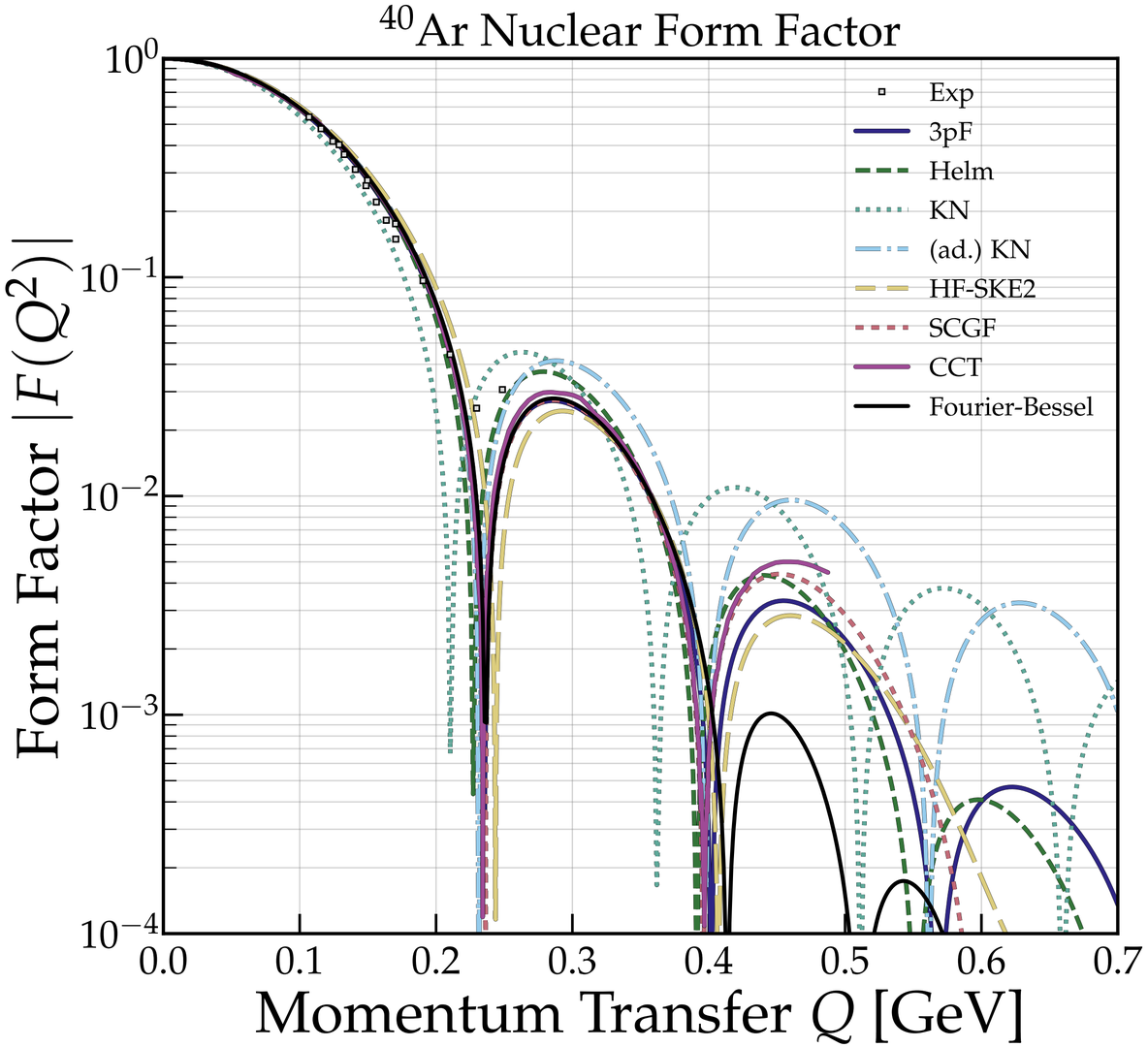

Argon Charged Form Factor

- Woods-Saxon 3-parameter Fermi
  De Vries et al. [Atom. Data Nucl. Data Tabl. 1987]
- Helm
  Helm [Phys. Rev. 1956]
- Klein-Nystrand: nuclear charge density distribution is modeled as a hard sphere with radius $(R_A)_{\mathrm{KN}} = 1.23\,A^{1/3}$ fm convoluted with a Yukawa potential with range $a = 0.7$ fm acting as a diffuse surface. The form factor is given by

$$F_{\mathrm{KN}}(Q^2) = \frac{3j_1(QR_A)}{QR_A}\frac{1}{1+Q^2a^2}\,.$$

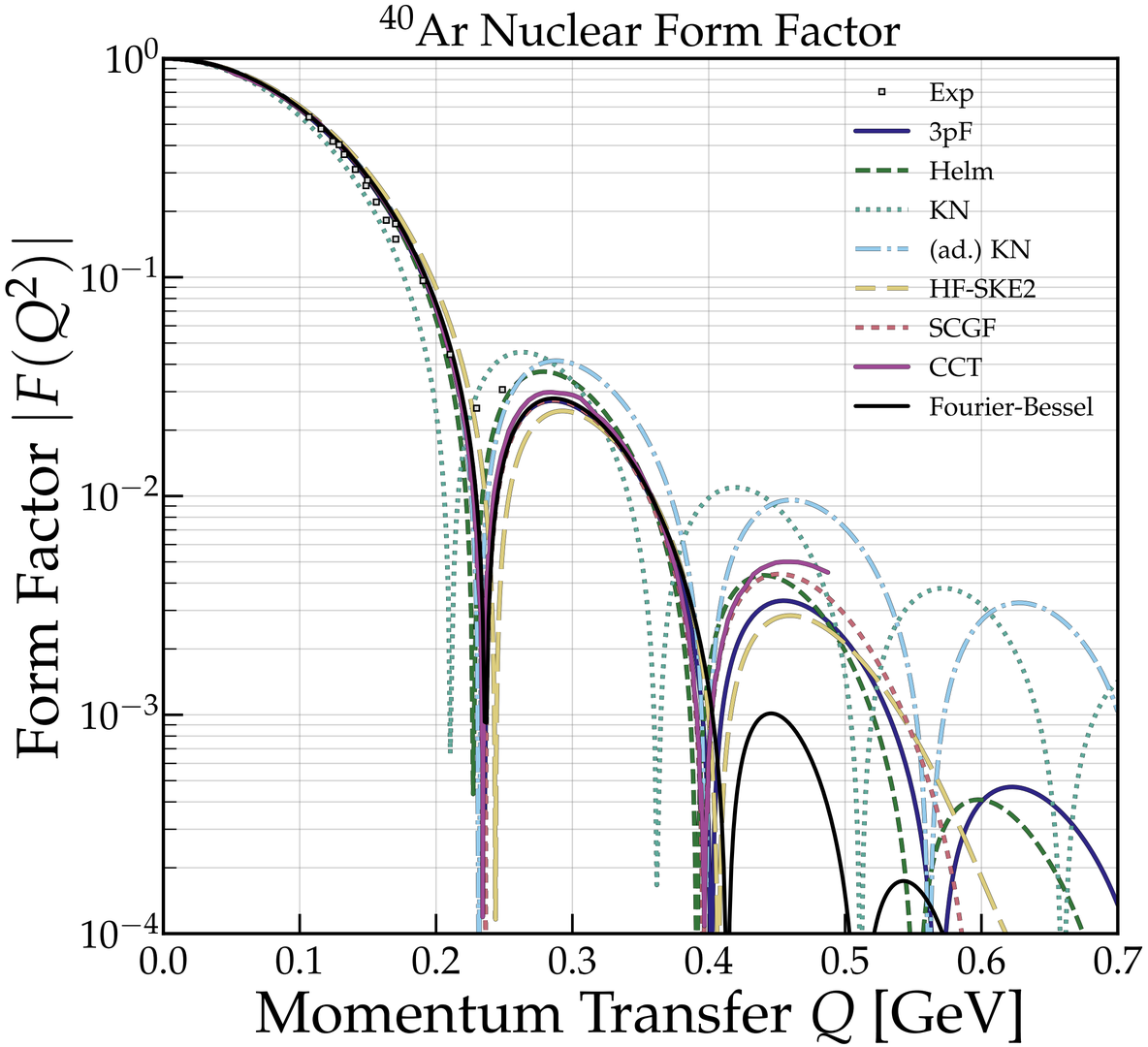

Argon Charged Form Factor

- Woods-Saxon 3-parameter Fermi
  De Vries et al. [Atom. Data Nucl. Data Tabl. 1987]
- Helm
  Helm [Phys. Rev. 1956]
- Klein-Nystrand
  Klein & Nystrand [9902259]
- Adapted Klein-Nystrand: same functional form as Klein-Nystrand but now

$$(R_A)_{\text{adKN}} = \sqrt{5r_0^2/3 - 10a^2}\ \text{fm},$$

with r_0 the measured proton rms radius of the nucleus. For ^{40}Ar, $r_0 = 3.427$ fm.

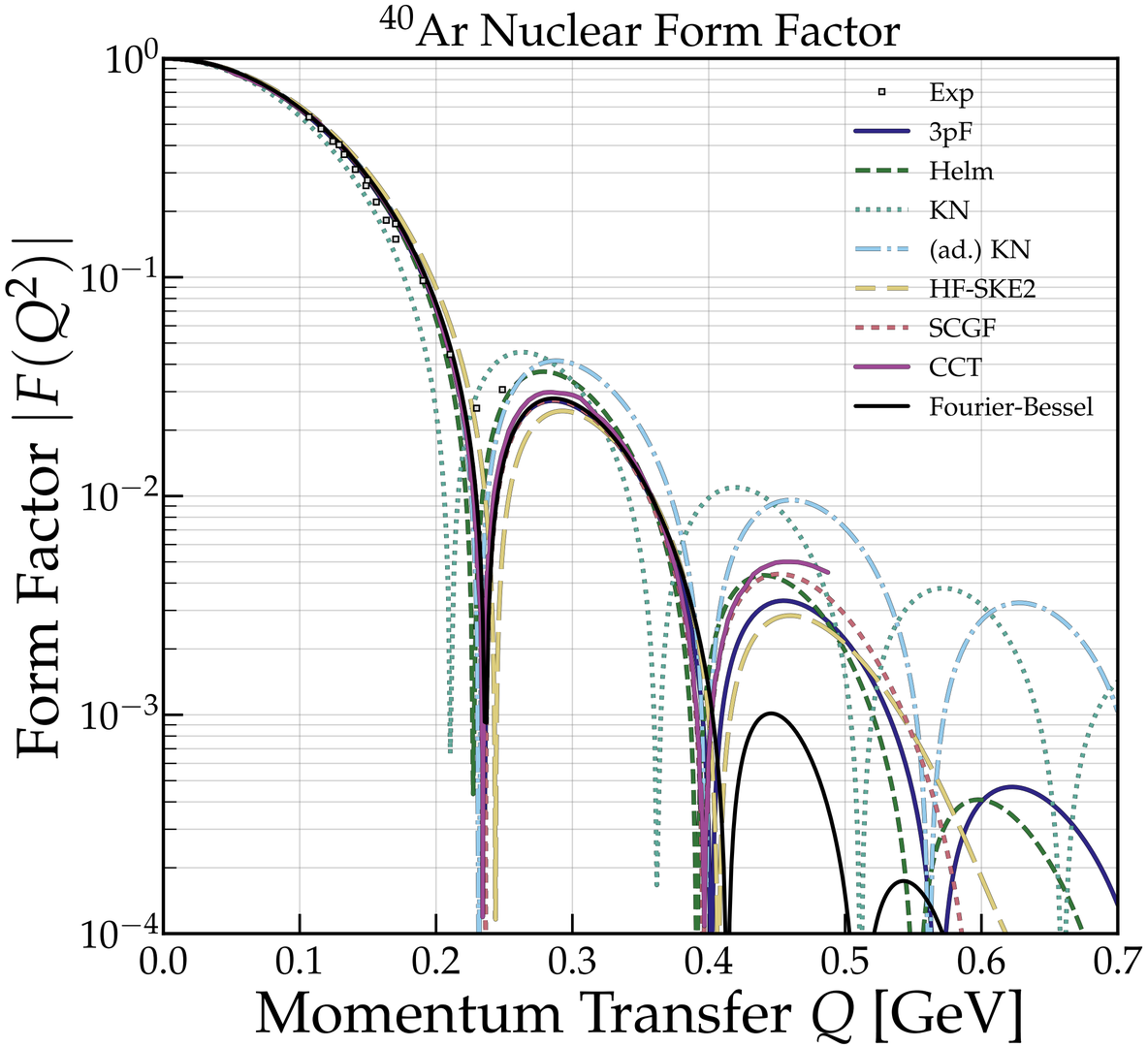

Argon Charged Form Factor

- Woods-Saxon 3-parameter Fermi
  De Vries et al. [Atom. Data Nucl. Data Tabl. 1987]
- Helm
  Helm [Phys. Rev. 1956]
- Klein-Nystrand
  Klein & Nystrand [9902259]
- Adapted Klein-Nystrand
  Papoulias et al. [1911.00916]
- Hartree-Fock with Skyrme: solve HF equations with a Skyrme nuclear potential to obtain single-nucleon wave functions for the bound nucleons in the nuclear ground state. Nuclear charge density distribution calculated from the proton wave function.

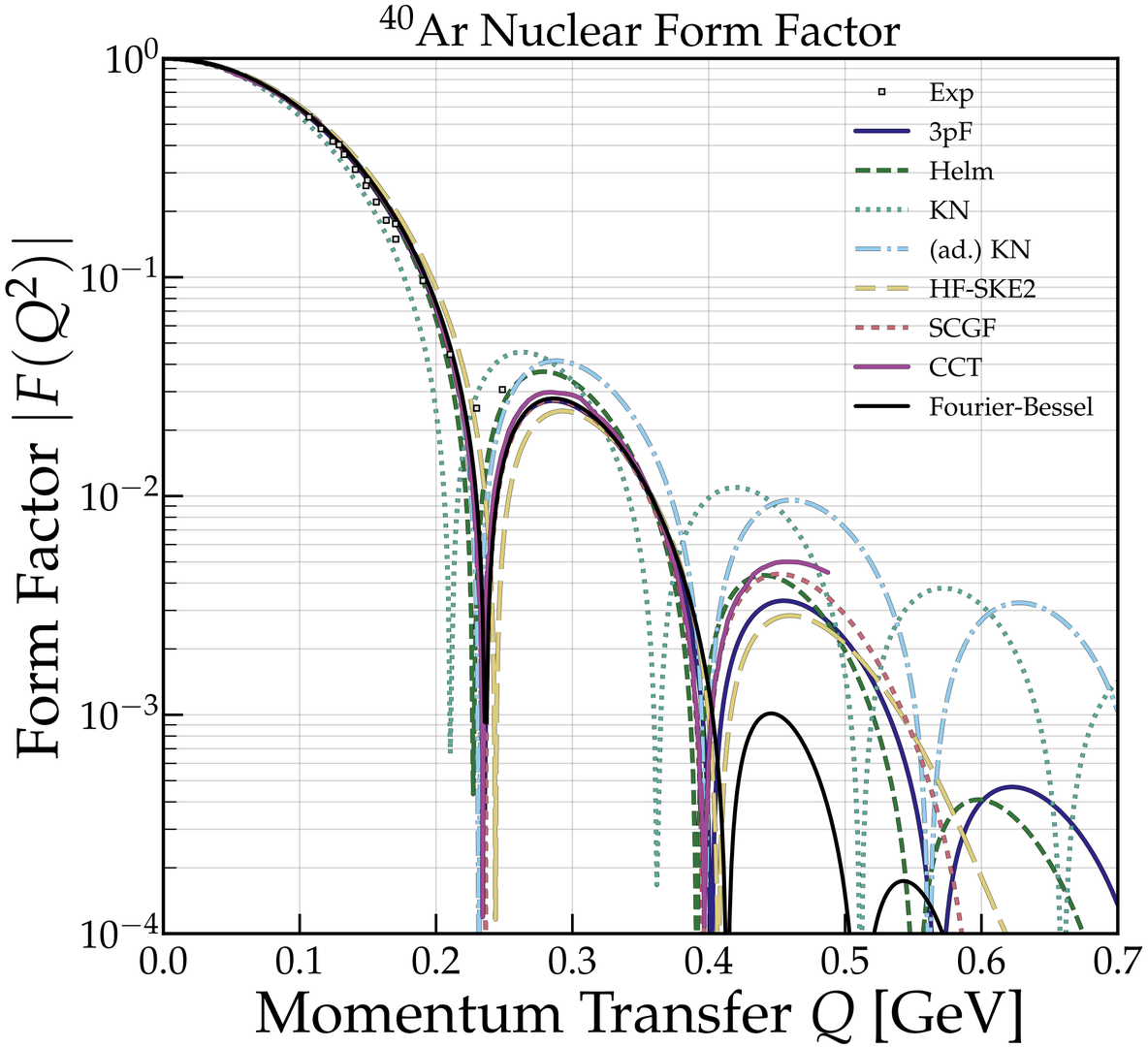

Argon Charged Form Factor

- Woods-Saxon 3-parameter Fermi
  De Vries et al. [Atom. Data Nucl. Data Tabl. 1987]
- Helm
  Helm [Phys. Rev. 1956]
- Klein-Nystrand
  Klein & Nystrand [9902259]
- Adapted Klein-Nystrand
  Papoulias et al. [1911.00916]
- Hartree-Fock with Skyrme
  Van Dessel et al. [2007.03658]
- Coupled-cluster Theory: use coupled-cluster theory to obtain the ground state of ^{40}Ar, Hamiltonian given by

$$\bar{H}_N = e^{-T} H_N e^{T}$$

where $T = T_1 + T_2 + T_3$ is the cluster operator and H_N is the Hamiltonian obtained from the next-to-next-to-leading order expansion in χEFT using the saturated chiral potential NNLO$_{\text{sat}}$.

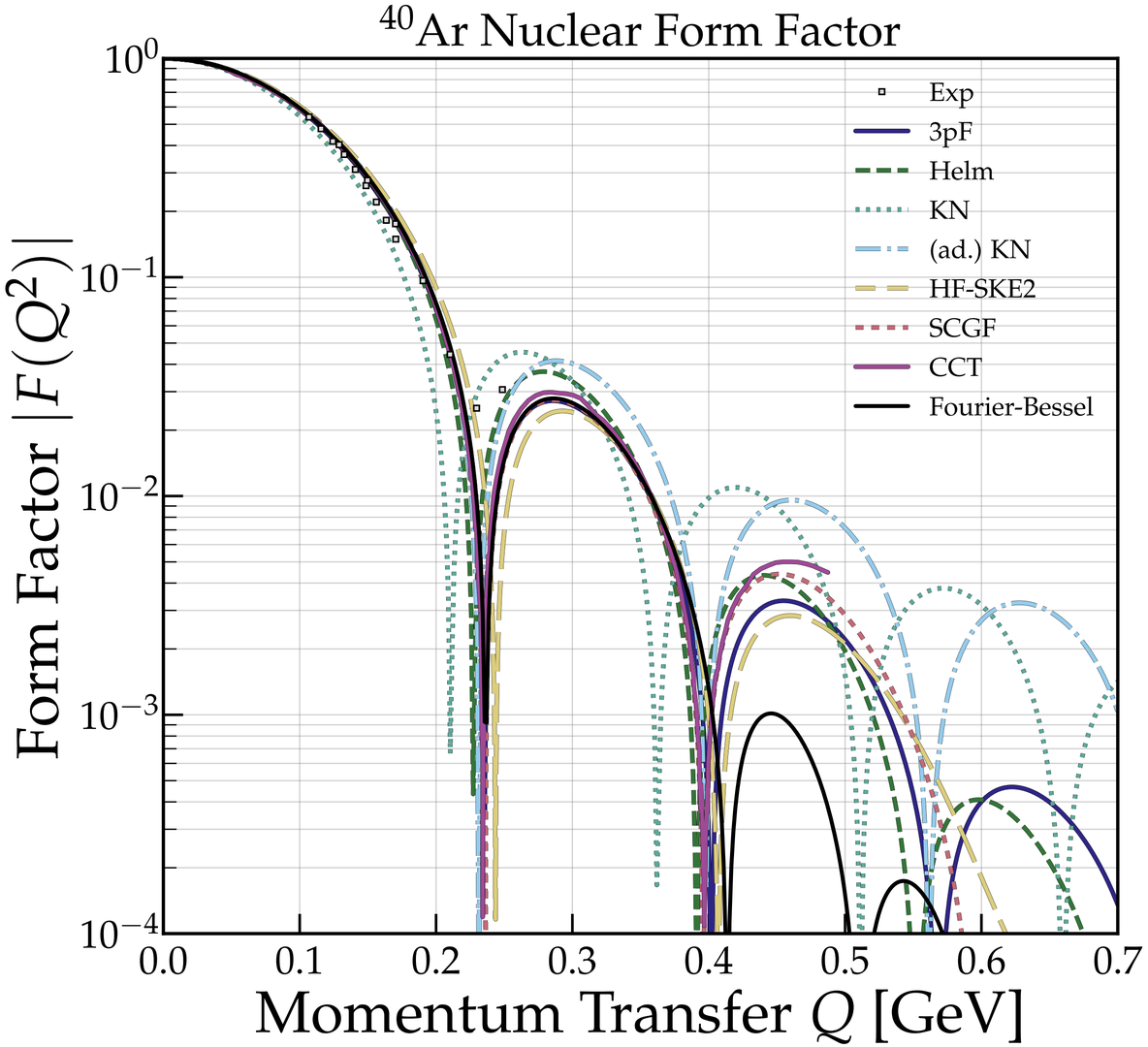

Argon Charged Form Factor

- Woods-Saxon 3-parameter Fermi
  De Vries et al. [Atom. Data Nucl. Data Tabl. 1987]
- Helm
  Helm [Phys. Rev. 1956]
- Klein-Nystrand
  Klein & Nystrand [9902259]
- Adapted Klein-Nystrand
  Papoulias et al. [1911.00916]
- Hartree-Fock with Skyrme
  Van Dessel et al. [2007.03658]
- Coupled-cluster Theory
  Payne et al. [1908.09739]
- *Ab initio* Self-Consistent Green's Function:

iteratively solve the Dyson equation to obtain the Green's function and use it to obtain the ground state of ^{40}Ar. The Hamiltonian is obtained from the next-to-next-to-leading order expansion in χEFT using the saturated chiral potential NNLO$_{\text{sat}}$.

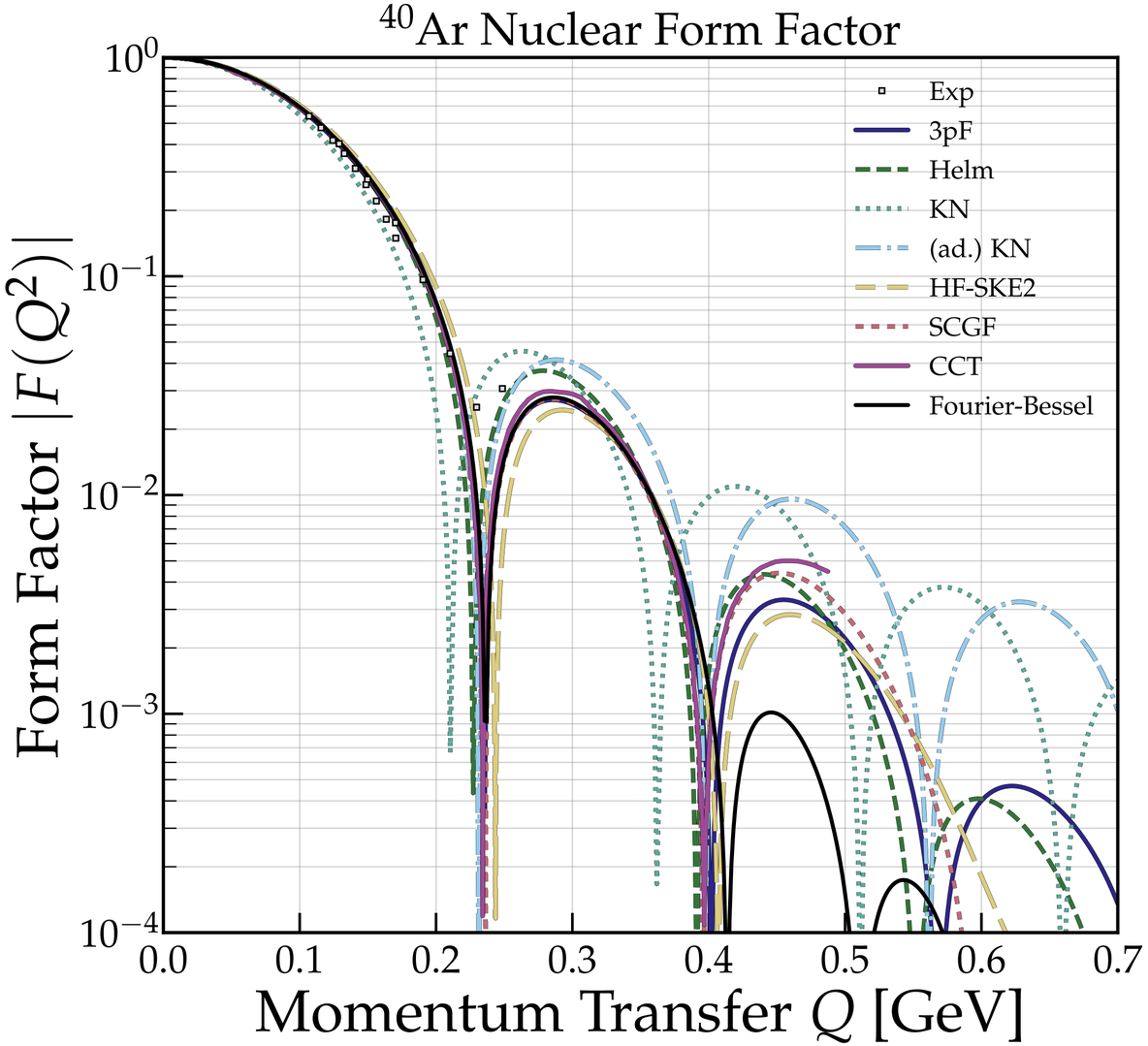

Argon Charged Form Factor

- Woods-Saxon 3-parameter Fermi
  De Vries et al. [Atom. Data Nucl. Data Tabl. 1987]
- Helm
  Helm [Phys. Rev. 1956]
- Klein-Nystrand
  Klein & Nystrand [9902259]
- Adapted Klein-Nystrand
  Papoulias et al. [1911.00916]
- Hartree-Fock with Skyrme
  Van Dessel et al. [2007.03658]
- Coupled-cluster Theory
  Payne et al. [1908.09739]
- *Ab initio* Self-Consistent Green's Function
  Barbieri et al. [1907.01122]
- Fourier-Bessel: use a Fourier-Bessel series expansion for the nuclear charge density distribution

$$\rho_N(r) = \begin{cases} \mathcal{N} \sum_n a_N^{(n)} j_0(n\pi r/R_N) & \text{for r} < \text{R}_\text{N} \\ 0 & \text{for r} > \text{R}_\text{N} \end{cases}$$

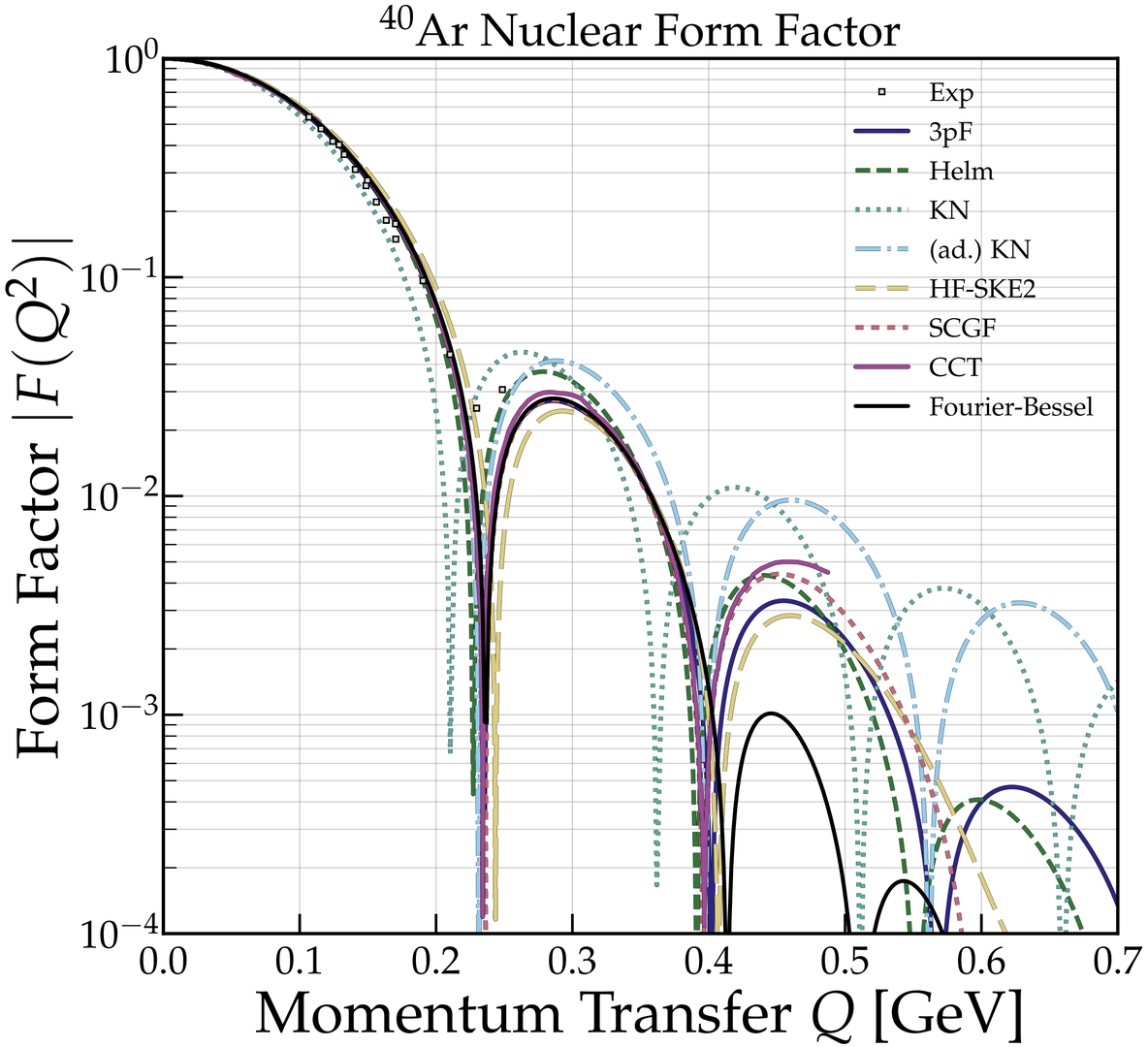

Argon Charged Form Factor